UniversitätsSpital Zürich

Klinik für Klinische Pharmakologie und Toxikologie

Direktor: Prof. Dr. med. Gerd A. Kullak-Ublick

Arbeit unter Leitung von Michele Visentin, Ph.D.

Cellular and molecular mechanisms of colistin-induced nephrotoxicity

INAUGURAL-DISSERTATION

zur Erlangung der Doktorwürde der Humanmedizin

der Medizinischen Fakultät

der Universität Zürich

vorgelegt von

Pascal Gantenbein

Genehmigt auf Antrag von Prof. Dr. med. Gerd A. Kullak-Ublick

Zürich 2018

Table of Contents

1 Abstract

Background: Colistin is a polypeptide antibiotic extensively used as a last resort agent in the treatment of multi drug resistant (MDR) Gram-negative bacteria. Its bactericidal potency is associated with nephrotoxic adverse effects that limit the use in clinical practice. Little is known about the exact mechanism of colistin-induced cellular damage, and efficient protective strategies are lacking.

Aim: To characterize the effect of colistin at the mitochondrial level and to explore the use of L-carnitine as a potential protective agent.

Methods: The impact of colistin exposure on mitochondria was evaluated in intact wild type HEK293 cells (WT-HEK293 cells) and in freshly isolated mitochondria from both WT-HEK293 cells and mouse kidney. The impact of intracellular L-carnitine on colistin-induced mitochondrial toxicity was evaluated in HEK293 cells stably transfected with the low affinity L-carnitine transporter SLC22A4 (OCTN1).

Results: We found that OCTN1-HEK293 cells had significantly higher intracellular levels of L-carnitine as compared with WT-HEK293 cells. After 48-hour exposure to colistin at an extracellular concentration of 100 μM, a marked mitochondrial membrane depolarization was induced in WT-HEK293 cells whereas mitochondria from OCTN1-HEK293 cells were not affected. Mitochondria exposed to colistin were rapidly shrunken and depolarized. Mitochondrial membrane depolarization was fully abolished by ADP, the most potent inhibitor of the mitochondrial permeability transition pore (MPTP). L-carnitine, recently reported as an inhibitor of the MPTP, failed to directly protect from the depolarization.

Conclusions: Colistin had a direct effect on mitochondrial function by inducing a rapid depolarization. The protective effect of ADP suggests that colistin-induced depolarization might be secondary to the opening of the MPTP. L-carnitine showed a protective effect towards mitochondria when cells were exposed to colistin, but not when isolated mitochondria were exposed to colistin, suggesting that L-carnitine protects mitochondria through an indirect mechanism.

2 Abbreviations

ADP	Adenosine diphosphate
AKI	Acute kidney injury
AMP	Adenosine monophosphate
ATP	Adenosine triphosphate
AUC	Area under the curve
BCA	Bicinchoninic acid
BSA	Bovine serum albumin
CPT	Carnitine palmitoyltransferase
DNA	Deoxyribonucleic acid
FADH	Flavin adenine dinucleotide
FBS	Fetal bovine serum
HEK-239	Human embryonic kidney cells 239
IMM	Inner mitochondrial membrane
MDR	Multi drug resistant
MIC	Minimum inhibitory concentration
MPTP	Mitochondrial permeability transition pore
NAD	Nicotinamide adenine dinucleotide
OCT	Organic cation transporter
OCTN	Organic cation transporter, novel
OMM	Outer mitochondrial membrane
PBS	Phosphate-buffered saline
R123	Rhodamine 123
RNA	Ribonucleic acid
SDHA	Succinate dehydrogenase complex flavoprotein subunit A
TOMM	Translocase of the outer mitochondrial membrane
WT	Wild type

3 Introduction

3.1 Antibiotic classification and mechanisms of action

Infectious diseases threaten humanity since ancient times. Whether we look at a deadly world-spanning pandemic caused by Yersinia pestis in the middle ages, at life-threatening meningococcal meningitis in newborns, or at cumbersome ubiquitous urinary tract infections in old age homes, the discovery and development of effective antimicrobial drugs have greatly improved our chances for survival and revolutionized modern medicine. While several hundred antibiotics are currently in clinical use, all act according to a few basic pharmaceutical mechanisms of action. Katzung et al defined two major groups of antimicrobial substances; “an antimicrobial substance that can eradicate an infection in the absence of host defense mechanisms and kills bacteria is classified as bactericidal; an antimicrobial drug that inhibits antimicrobial growth but requires host defense mechanisms to eradicate the infection and does not kill bacteria is labelled bacteriostatic” (Bertram G. Katzung, 2015).The bactericidal group includes the following classes: β-Lactam antibiotics, which are named after their chemical structures that contain a beta-lactam ring block the synthesis of bacterial murein, an essential component of bacterial membranes (Bertram G. Katzung, 2015). Subgroups contain the oldest of the commercially used antibiotics, the penicillins (e.g. penicillin G, aminopenicillin), its derivatives and, because of their excessive spectrum only very restrictively prescribed penems (e.g. carbapenem, meropenem) and the cephalosporins (e.g. ceftriaxon, cefepem) (Freissmuth, 2016). The sulfonamides (e.g. co-trimoxazole, trimethoprim) show efficacy against actinomycetes and chlamydia (acne, sexual transmitted diseases) by inhibiting the synthesis of tetrahydrofolic acid, which is important for the synthesis of DNA and RNA (Freissmuth, 2016). The polymyxins (e.g. polymyxin B, colistin), effective against Actinobacter, Pseudomonas aeroguinosa and Klebsiella (nosocomial infections) are known to disintegrate the outer bacterial membrane (Zavascki et al., 2007). Rifamycins (rifampicin), known for their efficacy against mycobacteria (tuberculosis, lepra), work by blocking parts of the RNA-synthesis (Rothstein, 2016). There are also antibiotics that hinder the protein synthesis of organells, making them bacteriostatic by slowing the metabolism of bacteria. They include the tetracyclins (e.g. doxycycline), used against bacteria without outer membranes like Borrelia (e.g. erythema migrans) (Chukwudi, 2016). The macrolides (e.g. clarythromycin, erythromycin) specifically alter bacterial ribosome function and

hinder protein synthesis, due to their penicillin-like efficacy they are often used as a substitute antibiotic for patients that are allergic to penicillin in gram-negative bacterial infections (Kwiatkowska and Maslinska, 2012). At least one agent of each of these groups has been added to the World Health Organization's List of Essential Medicines (WHO, 2015), underlining their indispensability for human health in the 21st century.

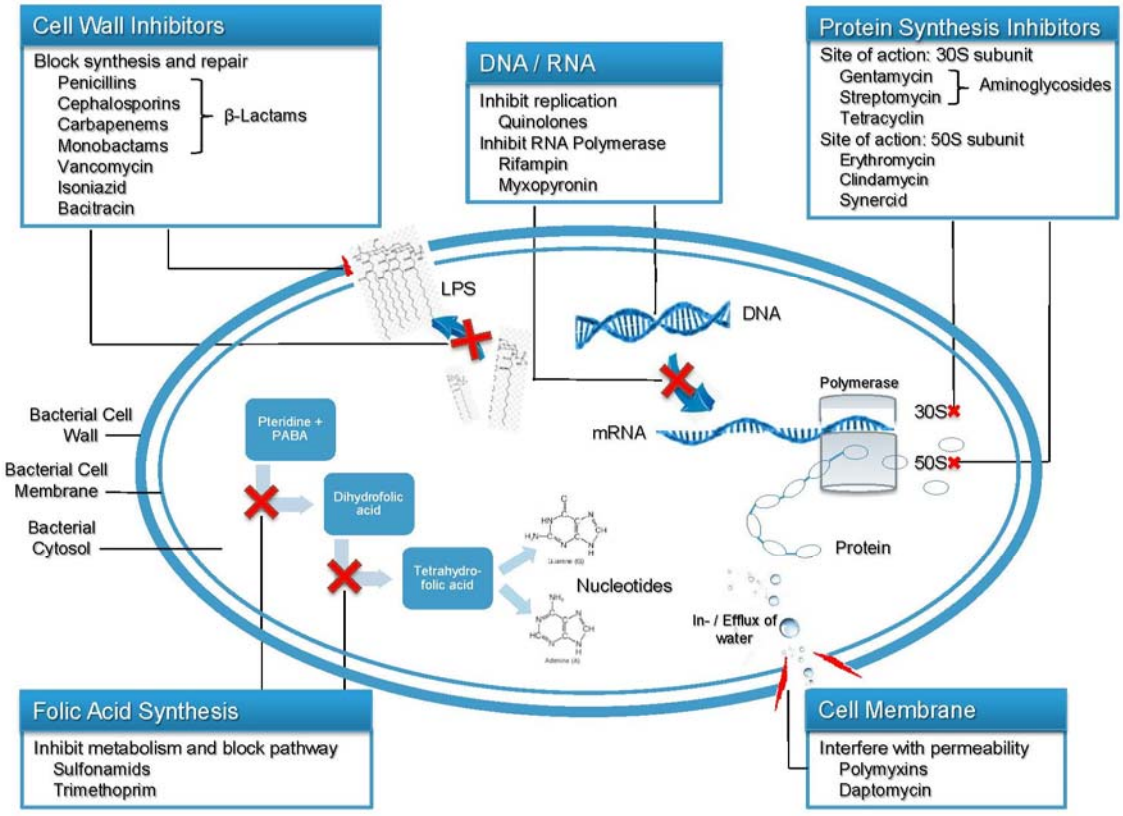

Figure 1. Different classes of antibiotics and their proposed primary mechanism of action on bacterial cells (adapted from Kapoor et al., 2017)

3.2 Bacterial infections in the post-antibiotic era

The overuse of antibiotics to feed animals and to treat non-bacterial and/or harmless infections, resulted in the selection of multidrug resistant (MDR) bacterial strains (Michael et al., 2014). Especially worrisome are MDR gram-negative infections (e.g. Pseudomans spp.) (Bergogne-Berezin and Towner, 1996). Due to the lack of effective new antibiotics, old, dismissed drugs are emerging as important weapons to fight MDR gram-negative infections.

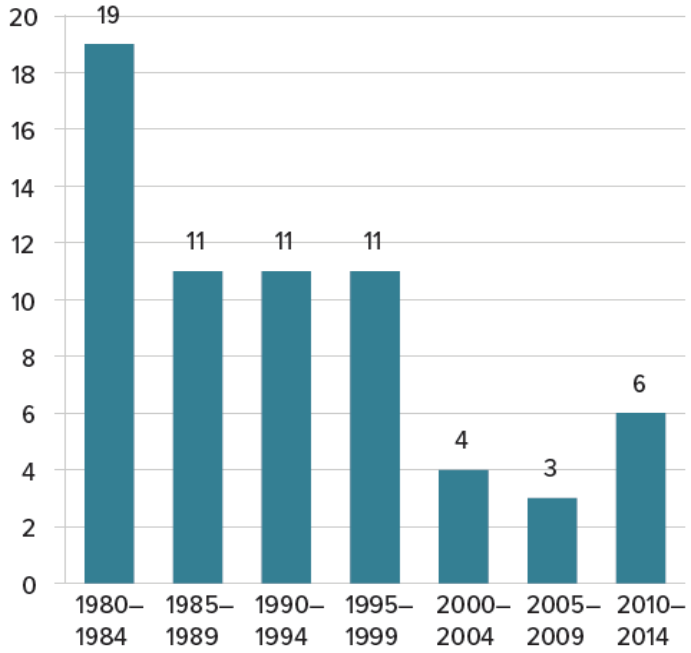

Figure 2. Comparison of numbers of new antibiotics developed and approved by the Food and Drug Administration (FDA) in the US since 1980. Only systemically administered agents are shown (Ventola, 2015).

For instance, vancomycin is back into clinical practice as an efficient antibiotic to treat methicillin-resistant Staphylococcus aureus (MRSA) (Nikaido, 2009). Another potent antibacterial agent rescued to “save the day” is colistin. Colistin was gradually dismissed from clinical use due to kidney toxicity (Koch-Weser et al., 1970).

Dosing of these old antibiotics are often not optimized through proper pharmacokinetic and pharmacodynamic studies. Not surprisingly, colistin administration protocols vary considerably among countries. Recent clinical studies pointed out, that colistin dosing should be much higher than the protocols currently in use suggest, to maximize the antibiotic activity. (Pogue et al., 2015).

3.3 Pharmacology of antibiotics

The goal of antibiotic treatment is to support the immune system in the battle against the germ. For an optimal response, the administered drug must reach and accumulate at the site of infection. Usual routes of administration of antibiotics are by ingestion or topical application. More severe cases and aggressive bacterial infections are treated systemically. Depending on the chemical and physical properties, some antibiotics, like penicillins and cephalosporins, are excreted through the kidneys (Barza and Weinstein, 1976; Christ, 1991), others, like macrolides, by the liver (Periti et al., 1989).

The therapeutic window is relatively small for a wide selection of antibiotic drugs. Hence the selection of an antimicrobial dosage regimen must be chosen also with respect to the physical status of the patient. The dosage is influenced by the relationship between target antimicrobial concentrations and the clinical outcomes of safety and efficacy. The minimum inhibitory concentration (MIC), used in the past to predict the drug efficacy, is now combined with the pharmacokinetic parameters of the same drug, also known as pharmacodynamics. Antimicrobial pharmacodynamic parameters are: (i) the peak concentration (C_{max}):MIC ratio, (ii) the area under the concentration-time curve (AUC):MIC ratio, and (iii) the percentage of time that the antimicrobial concentration remains above the MIC (T>MIC) (Levison and Levison, 2009). While the introduction of these parameters has improved the predictivity of antibiotic efficacy, the influence of other variables like (i) total versus free, (ii) blood versus tissue drug concentration, and (iii) interstitial versus intracellular concentrations in relation to the pathogen of interest make it difficult to optimize dosing for most antibiotics (Craig, 1998).

3.4 Antibiotic-induced nephrotoxicity

Kidney is often the limiting organ during antibiotic therapy; the damage often manifests with acute kidney failure and can be monitored by measuring the creatinine levels in the patient's serum. Several factors play a role in renal impairment, for instance a relatively high percentage of cardiac output flows through the kidneys exposing them to significant amounts of soluble drugs in the blood. Renal elimination is the result of three processes, the glomerular filtration, tubular reabsorption and tubular secretion.Both reabsorption and secretion are driven by a variety of facilitative transport systems that constitute the vectorial transport of solutes and drugs across the tubular epithelium (Apell, 2004). Such systems are finely tuned to maintain water, nutrients and electrolytes homeostasis, however, when it comes to xenobiotics, suboptimal transport often causes tissue injury. For instance, an asymmetrical vectorial transport towards the influx (influx > efflux) can occur, leading to anaccumulation of the drug in the proximal tubular cells. Alternatively, for antibiotics filtrated through the glomerulus into the primary urine, if the water reabsorption is not accompanied by a partial reabsorption of the drug, the higher relative concentration of the drug might become detrimental during passage through the loop of Henle and the distal tubuli. Intracellular accumulation can induce activation of apoptotic pathways or damage the

cell irreversibly leading to apoptosis or necrosis. Examples for this active accumulation include gentamycin, vancomycin and neomycin and are also suspected to play a role in the renal toxicity of the polymyxins. There is growing evidence that certain pathophysiological conditions alter the expression levels of many transporters with substantial pharmacological ramifications. Our group recently proposed that the long-standing observation that obese individuals are more susceptible to aminoglycoside-induced nephrotoxicity is due to the overexpression of the organic cation transporter 2 (OCT2), which mediates the transport of aminoglycosides from the blood stream into the proximal tubular cells (Gai et al., 2016). Other mechanisms of nephrotoxicity include mechanical damage through concentration dependent crystallization (ciprofloxacin) and inhibition of ion channels required for excretion of sodium and potassium (sulfamethoxazole-trimethoprim) (Pazhayattil and Shirali, 2014).

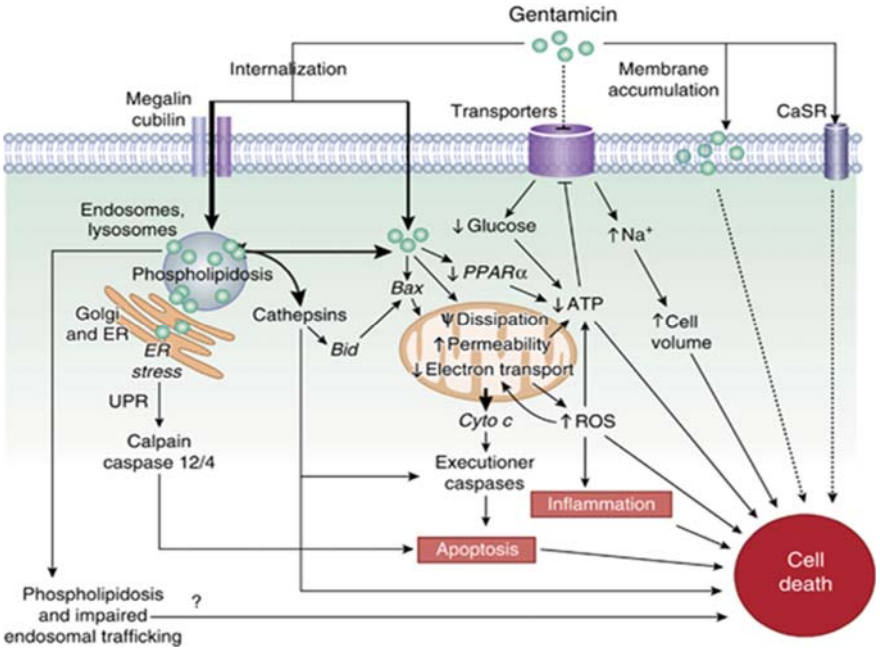

Figure 3. Proposed mechanisms underlying the cytotoxic effect of gentamicin, an aminoglycoside antibiotic notorious for its nephrotoxicity (Lopez-Novoa et al., 2011).

3.5 Colistin

Colistin, a polypeptide antibiotic of the polymyxin class, was discovered in the 1950s in Japan in Bacillus polymyxa and introduced into the clinic in the following decade (Kumazawa and Yagisawa, 2002). Its amphiphilic properties allow it to distribute well in polar and non-polar environments and ease its penetration through the outer bacterial membrane. According to Falagas et al. “Colistin displaces magnesium (Mg^{2+}) and calcium (Ca^{2+}) which normally stabilize the LPS molecules, from the negatively

charged LPS leading to a local disturbance of the outer membrane" (Falagas and Kasiakou, 2005). It is classified as a bactericidal antibiotic and is not bioavailable when taken orally and therefore usually administered intravenously (Kassamali et al., 2015). Colistin's clinical relevant antibacterial reach essentially includes Acinetobacter, with the most common strains A. baumanii, Acinetobacter genomic species 3, A. johnsonii and A. lwoffii (Bergogne-Berezin and Towner, 1996), MDR Pseudomonas aeruginosa and MDR Klebsiella infections (Koomanachai et al., 2007). The most commonly observed adverse events of colistin therapy are nephrotoxicity, mainly manifested as acute kidney injury (AKI) and mild neurotoxicity. Colistin seems to majorly accumulate in the renal cortex regions and its toxic effects on cellular level include heavy damage to mitochondria of kidney cells (Nilsson et al., 2015). One suspected mechanism of damage derives from the chemical structure of the polymyxins as they contain detergent d-aminobutyric acid and fatty acid chains that may induce leakage of the cell membrane (Falagas and Kasiakou, 2006). In bacteria, whose cell membranes are roughly comparable to human cellular membranes, this fatty acid chain is inserted into the membrane lipid bilayer leading to disruption of the membrane. As in bacteria, low cytoplasmic content of colistin in eukaryotic cells might be tolerated and interference compensated by the cells repair mechanisms. Higher cytoplasmic levels of the drug likely put too much stress on structural components of the double lipid layer membrane leading to their disintegration. The following uncontrolled passage of ions across the membrane influences the delicate osmotic homeostasis of the proximal tubular kidney cells and are probably a trigger to a cascade of signals that ends in apoptosis or necrosis of the cell. This hypothesis is merely based on the assumption, rather than any experimental evidence, that colistin can destroy the eukaryotic plasma membrane as well as it does with the bacterial membrane. Theoretical and experimental pitfalls of this hypothesis are: (i) bacterial membranes have a very different lipid composition (phosphatidylethanolamine and negatively charged lipids) as compared with eukaryotic cell membrane (mainly cholesterol), (ii) colistin is selectively toxic towards proximal tubular cells, (iii) red blood cells treated with colistin did not display signs of haemolysis (Mohamed et al., 2016). Yun and colleagues proposed, by using fluorescent-probed polymyxins, that the renal damage induced by polymyxins is exerted upon entering the cells (Yun et al., 2015). However, without knowing the mechanisms by which colistin enters cells, this question cannot be conclusively addressed. Colistin is extensively reabsorbed in the proximal tubule (Li et al., 2003).

Colistin is positively charged, thus diffuses poorly across the plasma membrane and therefore requires facilitative transport systems to cross the plasma membrane. Colistin clearance has been shown to be increased by co-incubation with other cations like tetraethylammonium (TEA) and the dipeptide glycine-glycine (Gly-Gly), indicating that the renal reabsorption of colistin may involve organic cation transporters and peptide transporters (Ma et al., 2009). Lu and colleagues recently found that the oligopeptide transporter 2 (PEPT2, SLC15A2) could transport [^{3}H]polymyxin B1 and that the uptake was reduced by co-incubation with colistin (Lu et al., 2016). Our group recently identified the carnitine and organic cation transporter 2 (OCTN2, SLC22A5) as novel transport system that recognizes colistin as a substrate and may contribute to the reabsorption of colistin at the apical side of proximal tubule cells (Visentin et al., 2017).

3.6 Mitochondrial physiology

Mitochondria are organelles representing the energy factory of most eukaryotic cells. According to the symbiotic theory, they arose from bacteria incorporated by an eukaryotic progenitor (Margulis, 1975). Indeed, mitochondria possess their own genetic material and still carry many bacterial features. Their prokaryotic origin is also considered the most likely explanation of mitochondrial toxicity induced by antibiotics. Mitochondria are characterized by two membranes; the outer mitochondrial membrane

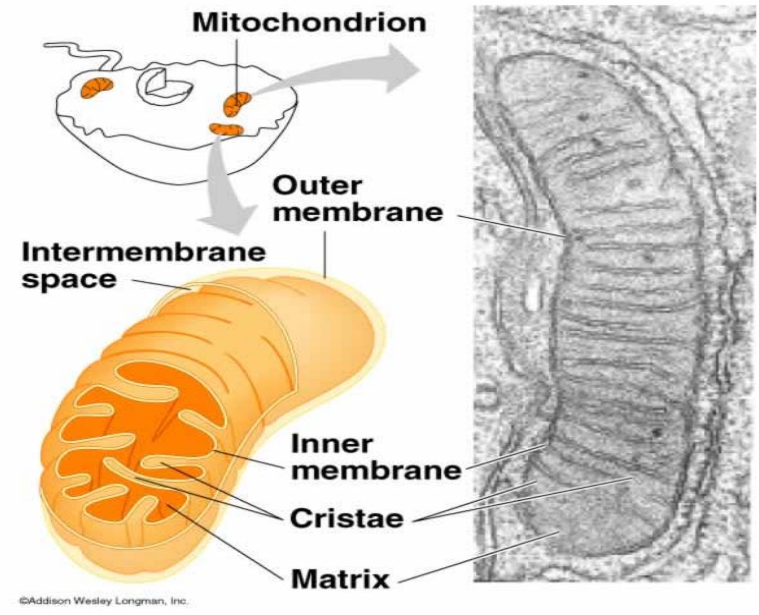

Figure 4. Basic model of human mitochondrial structure (left) and an electron microscope recording of mitochondria (right) (Denning, 2007).

(OMM) which is relatively permeable to small molecules, and the inner mitochondrial membrane (IMM), which is only very selectively permeable and contains a huge variety of intramembranous enzymes. In between lies the intramembranous space. The IMM encapsulates the mitochondrial matrix (Heidrich et al., 1970).

We previously defined mitochondria as the energy factory of the cell because one of the main task of mitochondria is to produce adenosine triphosphate (ATP), a substance whose dephosphorylation, the hydrolysis of ATP is strongly exothermic and is the main cellular energy source. Many biological processes are ATP-dependent (e.g. the movement of mysoin heads, the active transport of substances across membranes, tyrosine kinase signaling). In mitochondria, ATP is formed from ADP and inorganic phosphate (Pi) at the end of the electron transport chain by the ATP-synthase.

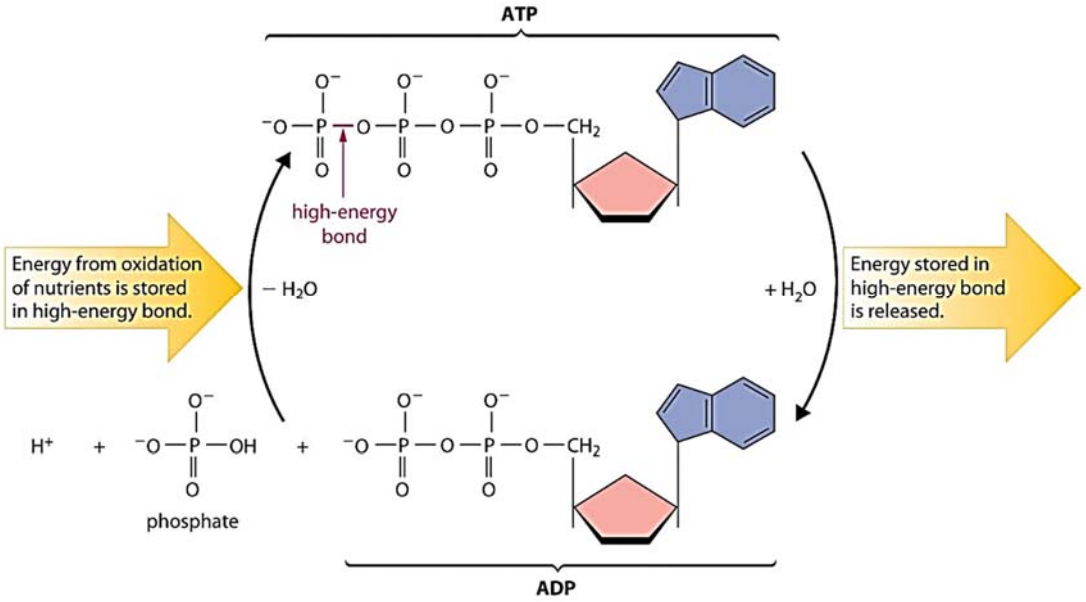

Figure 5. Depiction of ATP's chemical characteristics and its energy mediating capabilities (Averill, 2012).

Glucose, long chain fatty acids and amino acids can be used to produce ATP depending on the cell type or status. In the case of glucose, the first series of reaction occurs in the cytoplasm of the cell: anaerobic glycolysis yields 2 pyruvate, 2 ATP and 2 NADH molecules for each molecule of glucose. Pyruvate is converted to lactate in hypoxic conditions, like muscle cells during physical activity. When oxygen pressure is normal, pyruvate enters the citric acid cycle. Long chain fatty acids are activated into long chain acyl-Coa in the cytoplasm, then imported into the mitochondrial matrix via

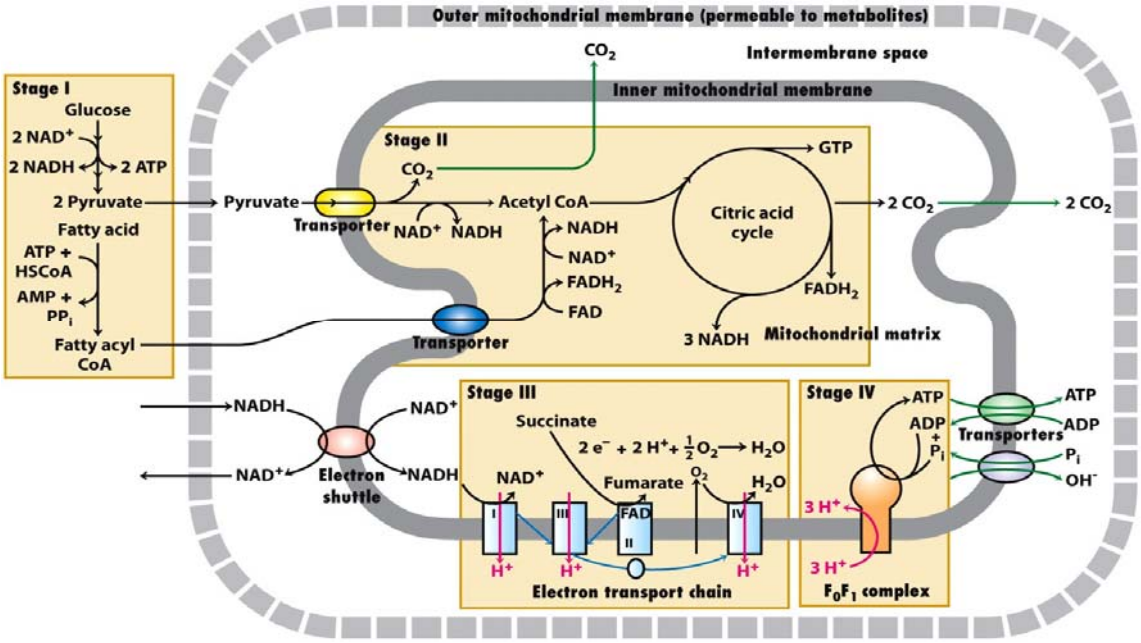

Figure 6. Overview of mitochondrial metabolism, the involved transporters and proteins (Freeman, 2008).

two specific transporters: the carnitine-palmitoyl-transferase I (CPT-I) localized on the OMM, and the carnitine palmitoyl-transferase II (CPT-II) in the IMM. In the matrix the activated fatty acid are metabolized to acetyl-CoA molecules by a series of reactions known as β-oxidation (Milane et al., 2015). In the glycolysis, the citric acid cycle and the β-oxidation, the electron carriers NADH and $FADH_2$ are generated. These carriers feed the electron transport chain, a series of 4 enzymatic complex integrated in the IMM that transfer electrons across the membrane to build a proton gradient, the driving force for a rotary turbine-like machine, the ATP-Synthase, which phosphorylates ADP to ATP (Jonckheere et al., 2012). Complex I, III and IV catalyze the oxidation of NADH to NAD^+, Complex II metabolizes Succinate to Fumarate, both resulting in an outwards directed relocation of protons in the intermembranous space (Milane et al., 2015; Berg 2018). In the oxidation of NADH and other processes taking part in the electron transport chain, electrons and part of oxygen atoms are combined to form elemental water. If the cell is hypoxic (low oxygen pressure), the electron transport chain cannot function properly leading to a cascade of detrimental events. In that case, various repair mechanisms are activated. However, if the disrupting cannot be fixed appropriately, apoptotic pathways can be triggered that ultimately lead to the cells death (Milane et al., 2015). The mitochondria itself is part of a complex network of regulatory pathways and biochemical sensors that work altogether to guarantee an

adequate production of ATP. An obvious and easy measurable parameter is the matrix concentration of ADP and AMP, which rises proportionally to the use of ATP and is accessed through the AMP-activated protein kinase (AMPK). Its activation leads to an upregulation of catabolic pathways which ultimately lead to an increased production of ATP (Mihaylova 2011). Depending on available substrates for the oxidative phosphorylation, oxygen levels and other factors, mitochondria can adjust their metabolic state into five different states of which each comes with differences in intramitrochondrial ADP levels, substrate levels and an altered membrane potential; as described by Chance and colleagues (Chance and Williams, 1955; Packer, 1960).

3.7 Mitochondria and the cell death machinery

Rasola and Bernardi defined mitochondria as a "firewall that controls the Ca^{++} concentration in the cell and in cytoplasmic microdomains by tuning the frequency of oscillatory Ca^{++} signals and by blunting the spread of cytosolic Ca^{++} waves" (Rasola and Bernardi, 2011). Mitochondria deal with transient cellular Ca^{++}-loads, relieving the cell from a burden that would otherwise jeopardize the cell integrity and most likely would lead to cell death. However, storing Ca^{++} can be detrimental for mitochondria as well, hence mitochondria are equipped with a fine system to release Ca^{++} upon reaching a certain threshold. The IMM rapidly increases its permeability to ions and solutes with molecular masses up to 1500 Dalton, a phenomenon called permeability transition (PT) achieved through a voltage-dependent channel sensitive to Ca^{++} (VDAC). This protein complex as been defined as the mitochondrial PT pore (MPTP). If the MPTP channel opens for a prolonged time, the resulting alteration of mitochondrial homeostasis and ion unbalance activates the intrinsic apoptotic pathway or even ends in primary necrosis of the cell if the residual cellular ATP is not sufficient to drive the apoptosis. The opening of the MPTP is eased also by oxidative stress, elevated phosphate concentration and adenine nucleotide depletion. The opening of an MPTP in one mitochondria might lead to a paracrine signal (Ca^{++} or other diffusible signals (e.g. superoxide sparks)) to the surrounding mitochondria and trigger the opening of other MPTPs (Halestrap, 2010; Rasola and Bernardi, 2011).

4 Aim

Colistin, a polypeptide antibiotic of the polymyxin class, has been increasingly reintroduced into clinical use in the last decades despite its notorious dose-limiting nephrotoxicity, due to the shortage of new antibiotics and the emergence of multidrug resistant bacteria. Current colistin therapy regimens are inconsistent, vary greatly between different healthcare providers and often cannot reach the target “therapeutic concentrations” due to nephrotoxicity. This approach reduces the efficacy of colistin and raises the incidence of drug resistant bug colonization. Optimal administration of colistin and proper management of the related adverse drug effects remain challenging, mostly because the pharmacology of this drug are still largely unknown. Although many risk factors for colistin-induced kidney injury have been identified, data supporting protective strategies that can buffer nephrotoxicity allowing to widen the therapeutic window of colistin, are mostly anecdotal.

Our group has recently found that mitochondria of mouse primary cultured proximal tubular cells exposed to colistin were fully protected by co-incubation with L-carnitine (unpublished data). L-carnitine supplementation would be a feasible and safe approach to modify colistin therapy and might represent a step forward towards the optimization of the treatment of multidrug resistant infections. To do so, the molecular mechanisms behind colistin-induced toxicity and L-carnitine protection need to be elucidated.

L-carnitine plays a pivotal role in mitochondria physiology by shuttling long chain free fatty acids from the cytoplasm into the mitochondrial matrix where they undergo β-oxidation, fueling electron transports, mitochondrial membrane potential and, in turn, ATP production. We hypothesized that L-carnitine protects from colistin-induced mitochondrial damage at two levels: (i) by reducing colistin intracellular accumulation by competing for OCTN2, (ii) by protecting the mitochondria.

The overall aim of this study was to assess the effect of intracellular L-carnitine on colistin-induced mitochondrial toxicity and investigate the mechanism behind L-carnitine mediated protection.

5 Materials and Methods

5.1 Reagents

ADP (Sigma)

Alexa Fluor 546 polyclonal goat anti-rabbit (Molecular Probes)

Colistin sulfate (Sigma)

Cyclosporin A (Sigma)

Dulbecco's modified Eagle's medium glucose 1g/L (DMEM, Gibco)

Fatty Free Bovine Serum Albumin (BSA, Sigma)

Fetal Bovine Serum (FBS, Gibco)

Gentamicin sulfate (Sigma)

G418 (Gibco)

HRP polyclonal goat anti-rabbit (abcam)

L-carnitine (Sigma)

L-carnitine [^{3}H] (Amersham)

Monoclonal rabbit anti-SDHA (Cell Signaling)

NucBlue Live ReadyProbes Reagent (ThermoFisher Scientific)

Penicillin (Gibco)

Phosphate Buffer (PBS, Kanton's apotheke)

Polyclonal rabbit anti-TOMM20 (Santa Cruz)

poly-D-lysine (Sigma)

Polyethylene Glycol 3,000 (PEG-3000, Sigma)

Rhodamine 123 (Sigma)

Streptomycin (Gibco)

Trypan Blue (Invitrogen)

Trypsin/EDTA 0.01% (Gibco)

Vancomycin (Sigma)

5.2 Buffer composition

Isolation buffer: 200 mM mannitol, 50 mM sucrose, 5 mM KH_2PO_4), 5 mM 3-(N-morpholino)propanesulfonic acid (MOPS), 0.1 % fatty acid free bovine serum albumin (BSA), 1 mM ethylene glycol-bis(β-aminoethyl ether)-N,N,N',N'-tetraacetic acid (EGTA), pH 7.15 titrated with KOH to pH 7.15.

Laemmli Buffer (loading buffer) 5x: 4 ml 1.5 M Tris-Cl pH 6.8, 10 ml glycerol, 2 g sodium dodecyl sulfate (SDS), 1 ml 1% bromophenol blue, pH 6.8, plus 15 mg per 1 ml 1,4-dithiothreitol (DTT)

Respiration buffer: 130 mM KCl, 5 mM KH_2PO_4, 5 mM 3-(N-morpholino)propanesulfonic acid (MOPS), 2.5 mM ethylene glycol-bis(β-aminoethyl ether)-N,N,N',N'-tetraacetic acid (EGTA), 3 mM succinate, 0.1 % bovine serum albumine (BSA), titrated with KOH to pH 7.15.

Running Buffer: 25 mM tris(hydroxymethyl)aminomethane (Tris), 190 mM glycine, 0.1% SDS, pH 8.3

Swelling buffer: 120 mM KCl, 10 mM tris(hydroxymethyl)aminomethane (Tris), 5 mM KH_2PO_4, titrated with HCl to pH 7.4

Transfer Buffer: 25 mM tris(hydroxymethyl)aminomethane (Tris), 190 mM glycine, 20% methanol, pH 8.3

Transport Buffer: 136 mM NaCl, 5.3 mM KCl, 1.1 mM KH_2PO_4, 1.8 mM $CaCl_2$, 0.8 mM $MgSO_4$, 11 mM D-glucose and 10 mM Hepes, titrated with Tris, pH 7.4

5.3 Cell Lines

Wild-type human embryonic kidney 293 cells (WT-HEK293) were maintained in Dulbecco's modified eagle's medium (DMEM) supplemented with 10% fetal bovine serum, 100 units/ml penicillin, 100 mg/ml streptomycin at 37°C in a humidified atmosphere of 5% CO_2. HEK293 cells stably transfected with the coding sequence of the organic cation transporter N1 (SLC22A4, OCTN1) were maintained in the same conditions as the WT-HEK293 cells and under selective pressure with 800 µg/mL

G418. Nearly confluent cells were rinsed with phosphate buffer (PBS), detached from the tissue culture plate by incubation (3 minutes at 37°C) with 0.01% trypsin/EDTA solution, then neutralized with growth medium. An aliquot of cell suspension was diluted 1:1 in 0.04% trypan blue solution andthe cells were counted by automatic cell counting (Countess, Invitrogen). Trypan blue dyes the damaged cells selectively, allowing discriminating between alive and dead cells. The density of alive cells was used to calculate the experimental seeding conditions. One portion of the cell suspension was re-plated for cell line maintenance.

5.4 Protein determination with bicinchoninic acid (BCA)

Protein content was measured colorimetrically with the commercially available kit Thermo Scientific™ Pierce™ BCA Protein Assay. Reagent A, containing the bicinchoninic acid, and reagent B, containing cooper (II) sulfate, were mixed (49:1). Two hundred microliters of the final solution were added to 25 µL of sample on a 96-well plate. The samples were incubated at 37 °C for 30 min then the absorbance at 560 nm was measured with the GloMax Multi Detection System (Promega). The nitrogen of the peptide bond reduces copper ions in alkalin conditions. The reduced copper is then chelated by two molecules of bicinchoninic acid generating a purple color. The intensity of the color is quantified by measuring the absorbance at 560 nm (Smith et al., 1985). A serial dilution of bovine serum albumin was used to produce a standard curve and the protein concentration was determined from the calculated experimental linear regression.

5.5 Rhodamine 123 staining, Immunostaining and confocal microscopy

WT-HEK293 and OCTN1-HEK293 cells were seeded at the density of $5x10^4$ cells/well on an 8-well open µ-slide chambered coverslip coated with 0.1 mg/mL poly-D-lysine. Lysine is a positively charged amino acid. The resultant net positive charge on the surface of the plastic dish eases and strengthens the cell adhesion through electrostatic interactions with the negatively charged phospholipid heads of the plasma membrane. This allows extensive washing and manipulation of the cell culture, with minimal risk of loss of cells through mechanical forces. For the Rhodamine 123 (R123) live staining, cells were incubated for 20 min with NucBlue® Live ReadyProbes® Reagent to stain the nuclei, washed with PBS, incubated for 20 min with 1 µM R123 in respiration buffer at room temperature, then washed again with PBS. For

immunofluorescence, cells were washed in PBS, permealized with 0.1 % Triton for 30 min and fixed at 37°C for 20 min with 4% Paraformaldehyde in PBS. Then they were blocked with 2% BSA in PBS at room temperature for 20 min. Cells were then probed overnight for TOMM20 (1:500) at 4°C. Afterwards, cells were washed with PBS, and incubated with Alexa 546-anti-rabbit (1:100) at room temperature for 30 minutes, washed with PBS and mounted with DAPI. All images were acquired with a confocal microscope (Leica DMI6000B).

5.6 Measurement of intracellular ATP content

For ATP measurement, CellTiter-Glo® 2.0 Cell Viability Assay was used. Cells were lysed with a lysis buffer provided by the kit. The ATP-release triggers the mono-oxygenation of luciferin by the enzyme luciferase, which generates a chemiluminescent signal that is proportional to the amount of ATP present. WT-HEK293 cells were seeded in 96-well plates at a density of $1x10^4$ cells/well in growth medium and incubated at 37°C in a humidified atmosphere of 5% CO_2 overnight. Afterwards, cells were exposed to the different drugs for 6 h at 37°C in a humidified atmosphere of 5% CO_2. The treatment was stopped by aspirating the medium and lysing the cells in Promega CellTiter-Glo® 2.0 buffer. Forty µL of each well were then transferred to a new 96-well plate and serial dilution of a standard solution of ATP was used to evaluate the linear correlation between chemiluminescent signal and ATP concentration. Data were normalized for the protein content measured as previously described.

5.7 Isolation of functional mitochondria

For isolation of functional mitochondria from cell culture, WT-HEK293 cells were grown to 85-95% confluence on 500 cm^2 tissue culture plates at 37 °C in a humidified atmosphere in 5% CO_2. To harvest, cells were washed 3 times with cold PBS, re-suspended in 10 mL of cold isolation buffer (IB) and transferred in 50 mL Sorvall centrifuge tubes. Cell suspension was then centrifuged in a SS34 rotor (Sorvall) for 10 min at 4°C at the speed of 2000 rpm. The pellet was re-suspended in 3.5 mL cold IB and homogenized in a 5 mL Teflon homogenizer at 1600 rpm. The homogenization speed is critical to destroy cells/tissues without damaging the mitochondria. For isolation of functional mitochondria from mouse kidney, the mouse was sacrificed; the kidneys were excised and homogenized as described above. The homogenate was

then centrifuged in a SS34 rotor for 5 min at 4 °C at 3000 rpm to separate nuclei and unbroken cells (pellet) from intracellular compartments (supernatant). The pellet was kept at -20°C until use. The supernatant was further centrifuged in a SS34 rotor for 10 min at 4 °C at 10000 rpm. The pellet was re-suspended and transferred into a 1.5 mL tube and spun down for 10 min at 4 °C at 10000 x g_{av}.The pellet containing the mitochondria was used immediately for functional assays (R123 uptake or swelling experiment) or kept at -20°C for western blot. The supernatant was ultra-centrifuged in a Centrikon T-1170 centrifuge for 1 hour at 4 °C at 100000 x $g_{av}$and the pellet was stored at -20°C for western blot analysis.

5.8 Western blot

The western blot consists of three main steps:

1. Separation of the protein according to the molecular weight. To separate the proteins onto a 12% polyacrylamide gel, 8 ml of Acrylamide Bis 30% were combined with 6.8 ml of deionized water, 0.2 ml of Ammonium persulfate (APS) and 0.015 ml of N,N,N',N'-Tetramethylethylendiamin (TEMED). The APS and TEMED induce the radical reaction that lead to the polymerization into a mesh-like structured gel. To ensure all samples starting the separation at once, a stacking gel (4.2 ml of deionized water, 0.9 ml Acrylamide Bis 30%, 0.07 ml of APS and 0.011 ml of TEMED) was prepared and poured on top of the resolving gel. Forty µg of protein were re-suspended in Laemmli buffer, de-naturated at 85°C for 15 minutes and loaded into the stacking gel. The presence of the anionic surfactant sodium dodecyl sulfate (SDS) in the Laemmli buffer overlays the proteins and leads to formation of negatively charged complexes whose charge correlates roughly with the size of the protein (Smith, 1994). This guarantees separation is based solely on size of the protein independent from their respective charge. By applying an electric field (150 V); the proteins migrate from the negative to the positive pole. The bigger the protein, the slower is the migration through the gel. The protein separation was monitored by co-running a pre-stained protein ladder (marker), a mixture of 9 proteins with different sizes. As soon as the smallest and therefore fastest proteins of the marker reached the other end of the gel, the run was stopped by discontinuing the electric flow.
2. Transferring of the separated protein on a membrane. The gel was “sandwiched” together with a PVDF membrane previously activated by soaking in methanol. The

surface of the PVDF membrane is strongly hydrophobic and would not bind the proteins if directly exposed to the aqueous transfer buffer. The “sandwich” was immersed in transfer buffer and an electric field (250 mA) was applied for ~ 1h to transfer the proteins from the gel onto the membrane. The negatively charged protein fractions will then migrate along the electric potential difference from the gel onto the membrane. The complete transfer of the marker onto the membrane serves as control of a successful transfer of the proteins.

3. Probing of the membrane with a certain antibody to detect the protein of interest. The membranes were blocked for 1 hour at room temperature or overnight at 4°C with 5% nonfat dry milk and 0.1% Tween-20 in PBS (blocking buffer). Afterwards the membranes were incubated for 1h with the desired primary antibody diluted in blocking buffer, then washed three times with blocking buffer, followed by 1h incubation with the appropriate horseradish peroxidase conjugated secondary antibody diluted in blocking buffer as well and 3 washing steps in blocking buffer and 2 washing steps with PBS-T.

5.9 Measurement of Rhodamine 123 uptake in isolated mitochondria

Rhodamine 123 (R123) is a lipophilic dye that specifically accumulates in mitochondria depending on the mitochondrial membrane potential and those chemical agents that collapse membrane potential (e.g. uncoupler, complex inhibitors) prevent uptake of R123 by mitochondria (Chen, 1988). R123 uptake can be monitored in non-quenching or quenching mode.

To measure the uptake of R123 in isolated mitochondria, R123 was dissolved in respiration buffer to a final concentration of 10 µM. The fluorescence emission at 538 nm of the R123 solution was measured, then a 5 µL aliquot of isolated mitochondria was mixed into the R123 solution and the decline of fluorescence intensity at 538 nm was monitored over the time. The accumulation of R123 leads to its aggregation which induces a red shift of fluorescence and extensive quenching of the emission at 538 nm (Perry et al., 2011). Loss in fluorescence signal in presence of mitochondria is considered an indicator of intact mitochondrial membrane potential (Emaus et al., 1986).

5.10 Assessment of mitochondrial swelling

An increase in volume of the isolated mitochondria leads to a macroscopic dilution of light absorbing substances in the mitochondrial matrix while a decrease in volume leads to a relative concentration of light absorbing substances. This phenomenon can be exploited to understand the effect of drugs on the morphologic state of the mitochondria. Isolated mitochondria were resuspended at the final concentration of 0.25 mg/mL in swelling buffer containing the different compounds to test and the absorption at 560 nm was measured with GloMax® Spectrophotometer (Promega).

5.11 Transport assay in intact cells

WT-HEK293 and OCTN1-HEK293 cells were seeded at a density of $1,5x10^5$ on 35-mm dishes coated with 0.1 mg/ml poly-D-lysine and incubated at 37°C in a humidified atmosphere in 5% CO_2 until 85-95% confluence was reached. The medium of the WT-HEK293 and OCTN1-HEK293 cells was aspirated and the cells were washed and equilibrated with pre-warmed transport buffer. Afterwards, transport buffer containing [^{3}H]L-carnitine was added. Uptake was stopped by quick aspiration followed by extensive washing with ice-cold transport buffer. Subsequently, cells were lysed with 1 ml of 1% Triton x100 for 40-50 minutes and 500 μl were mixed with 3 ml of scintillation liquid and assessed for intracellular radioactivity with a scintillation counter (Canberra Industries). Twenty-five microliter of the remaining solution were assessed for protein determination as previously described.

5.12 Statistical analysis

Statistical comparisons were performed from at least three independent measurements, using GraphPad Prism (version 5.0 for Windows, GraphPad Software).

6 Results

6.1 Uptake of L-carnitine in WT-HEK293 cells and OCTN1-HEK293 cells

Data from our group (Visentin et al., 2017) showed full protection of primary cultured proximal tubular cells from the toxic effects of colistin when co-incubated with L-carnitine. L-carnitine and colistin share the same transport system, OCTN2, however such protection might be only partially ascribed to the interaction at the OCTN2 level. To understand the impact of intracellular L-carnitine on colistin-induced toxicity, we exploited the substrate specificity of OCTN1. OCTN1 does not interact with colistin (Visentin et al., 2017) and is a low affinity transporter for L-carnitine (Yabuuchi et al., 1999). The uptake of [^{3}H]L-carnitine in WT-HEK293 cells was compared with that in OCTN1-HEK293 cells. Cells were incubated for 10 minutes with [^{3}H]L-carnitine at the extracellular concentration of 1 μM, a concentration that resembles that of the growth medium (Baker et al., 1988). As illustrated in figure 7, the intracellular level of [^{3}H]L-carnitine was notably higher in the OCTN1-HEK293 cells as compared with the WT-HEK293 cells (17.72 ± 3.2 vs 24.96 ± 4.2, P=0.03).

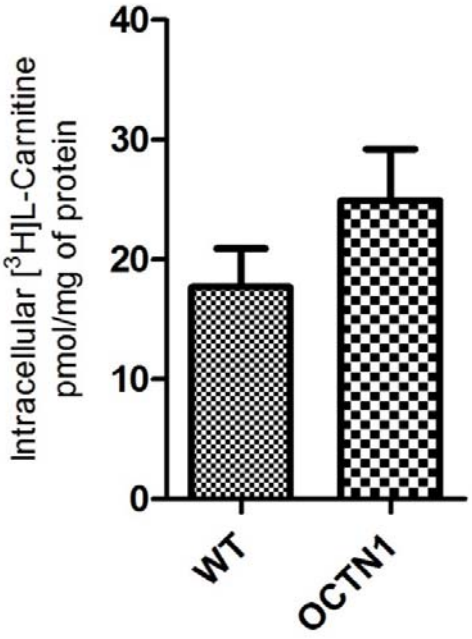

Figure 7. Uptake of [^{3}H]L-carnitine in WT- and OCTN1-HEK293 cells. Cells were exposed for 10 minutes to [^{3}H]L-carnitine at the extracellular concentration of 1 μM. Data represent the mean ± S.D. from three independent experiments.

6.2 Effect of colistin on mitochondrial membrane potential and mitochondrial integrity

We demonstrated that OCTN1-HEK293 cells had a higher intracellular level of L-carnitine. If intracellular L-carnitine could protect from colistin-induced toxicity, cells overexpressing OCTN1 would be more resistant to colistin than the respective wild-type cells. WT-HEK293 and OCTN1-HEK293 cells were exposed for 48h to colistin at an extracellular concentration of 100 μM then stained with 1 μM R123. The ability of mitochondria to generate and sustain a membrane potential across the inner membrane is the pre-requisite for mitochondrial function and cell survival. R123 specifically accumulates in mitochondria depending on the mitochondrial membrane potential (Chen, 1988). When the MMP collapses, R123 accumulation is inhibited.

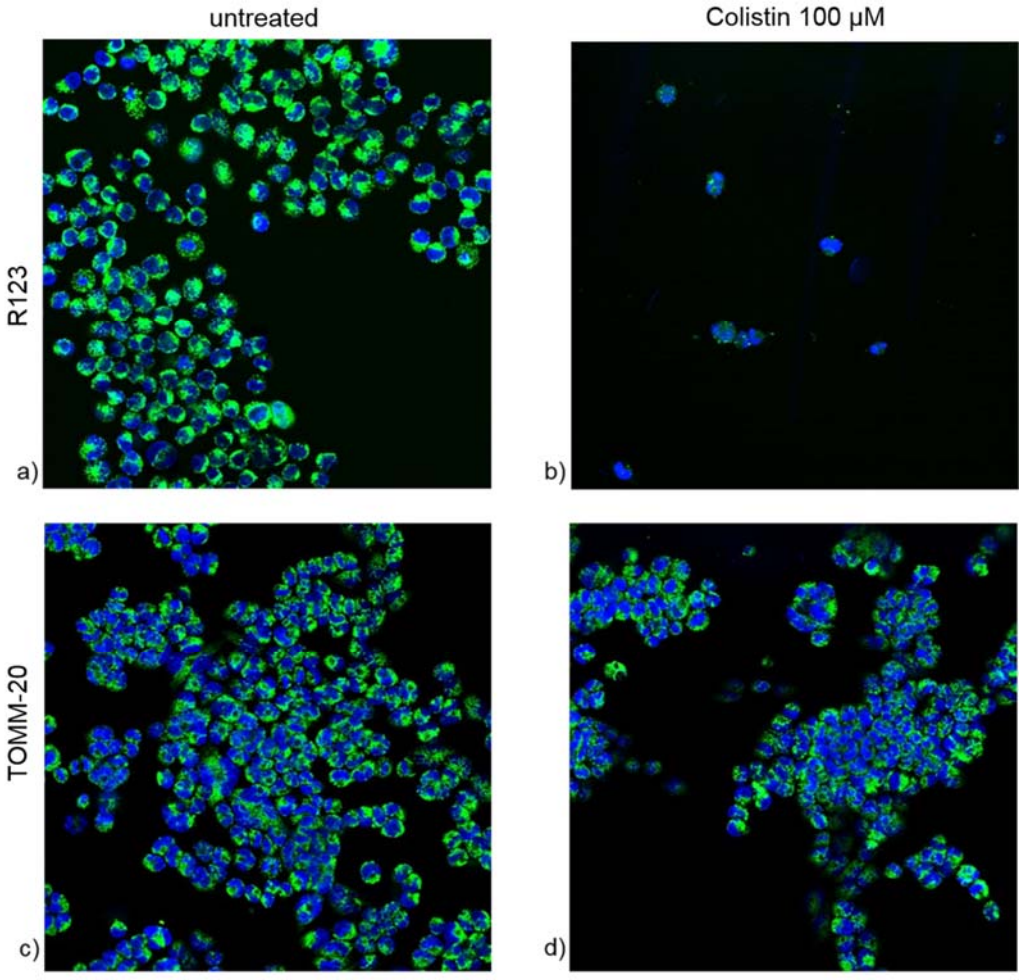

Figure 8. Colistin-induced mitochondrial damage in WT-HEK293 cells. WT-HEK293 cells were exposed to colistin at an extracellular concentration of 100 µM for 48 hours. Representative R123 staining (a and b) and TOMM-20 immunofluorescence (c and d).

Figure 8 shows that colistin exposure induced a marked reduction of the R123 green fluorescent signal, indicating mitochondrial membrane depolarization. In parallel, cells were probed for TOMM-20, a mitochondrial import receptor subunit that localizes on the mitochondrial outer membrane, to evaluate the impact of colistin on mitochondrial membrane integrity. It can be seen that in cells exposed to colistin, the TOMM-20 signal was similar to that from the untreated cells, suggesting that mitochondria integrity was not affected by colistin. Figure 9 shows that colistin exposure did not affect either R123 or TOMM-20 signal in OCTN1-HEK293 cells, suggesting that mitochondrial function and integrity were maintained.

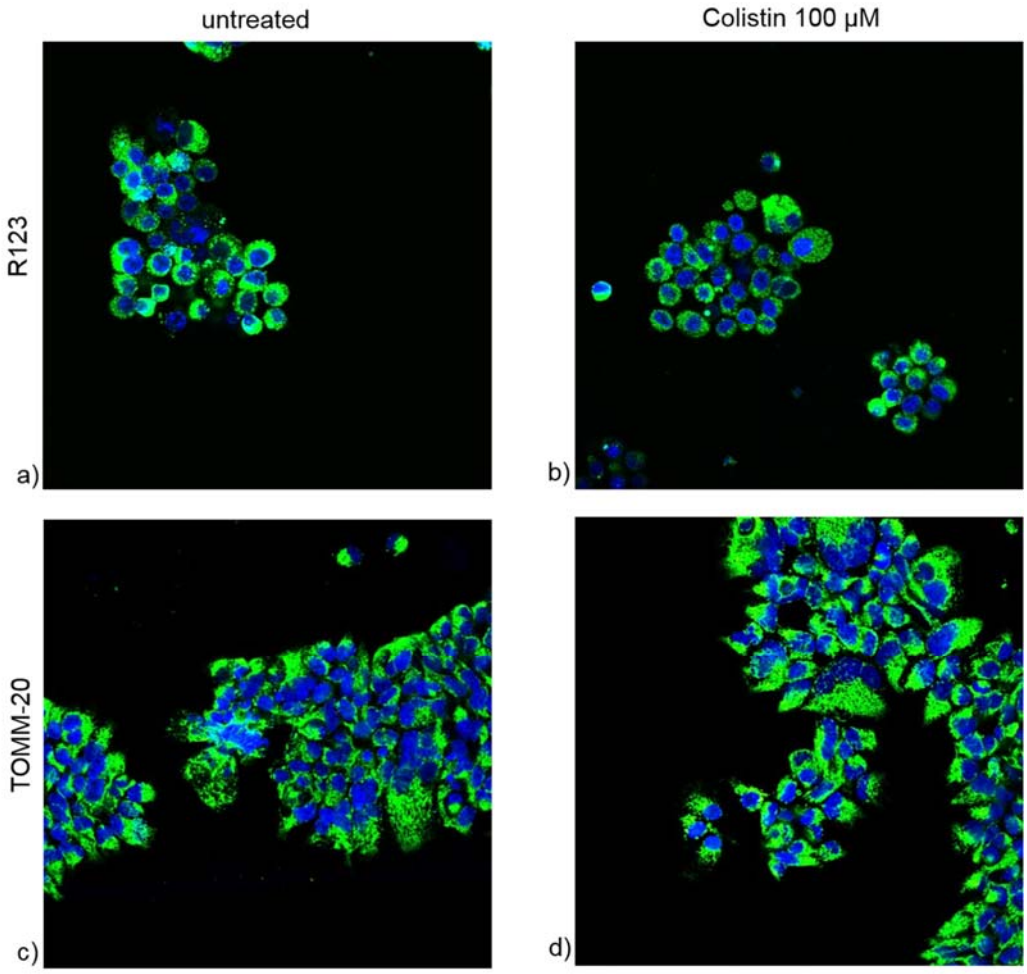

Figure 9. Mitochondrial toxicity induced by colistin. OCTN1-HEK293 cells were exposed to colistin at an extracellular concentration of 100 µM for 48 hours. Representative r123 staining (a and b) and TOMM-20 immunofluorescence (c and d).

6.3 Functional assessment of isolated mitochondria from WT-HEK293 cells

To understand whether the mitochondrial dysfunction (Figure 8) was the primary and central effect of colistin exposure, or rather a secondary one in a chain of damage events, we set up a method to test the direct effect of colistin on the function of isolated mitochondria. Mitochondria were enriched through different centrifugation steps (Frezza et al., 2007). The mitochondrial fraction enrichment was evaluated by Western blot. From the subcellular fractionation 3 pellets were collected. As mitochondrial marker we used the mitochondrial import receptor subunit (TOMM-20) and the succinate dehydrogenase complex flavoprotein subunit A (SDHA), which are localized at the outer and inner membrane, respectively. Figure 10 shows that both TOMM-20 and SDHA signals were detected in pellet 1, indicating that the mitochondria were successfully enriched in a single fraction. It can be seen that TOMM-20 was also partially detected in the pellet 3, likely as result of a contamination from broken mitochondria. Pellet 1 was used for further experiments in isolated mitochondria. The mitochondrial fraction was assessed for membrane potential and proton gradient by R123 uptake in isolated mitochondria. Mitochondria at a final concentration of 0.25 mg/ml were mixed with 10 μM R123 solution and the decline of fluorescence was monitored. R123 fluorescence spectrum shifts to the red in response to mitochondria energization (self-quenching) leading to a decreased emission at 538 nm (Emaus et al., 1986). The control is represented by the fluorescence intensity before the mitochondria were added. There is an empirical linear relationship between fluorescence intensity change and membrane potential (Chen, 1988). Figure 11 shows that untreated mitochondria induced a rapid decrease of fluorescent signal, suggesting a healthy state of the mitochondrial membrane potential. When mitochondria were exposed to the mitochondrial uncoupler Na-Salicylate, the fluorescence quenching was trivial as result of a collapsed membrane potential. Mitochondrial uncouplers are protonated weak lipophilic acids (A^-H^+) that dissolve in the inner membrane and diffuse through the lipid phase into the matrix compartment where they dissociate into the acid anion (A^-) and H^+, thereby dissipating the proton gradient (Smith and Moses, 1960). However, they do not accumulate in the matrix because their anion is also soluble in the lipid phase due to the charge delocalizing over their aromatic ring. The acid anion is expelled from mitochondria down the gradient of membrane potential (more positive

outside), thereby dissipating the gradient. This futile proton-shuttling cycle is repeated until there is no more gradient across the inner membrane.

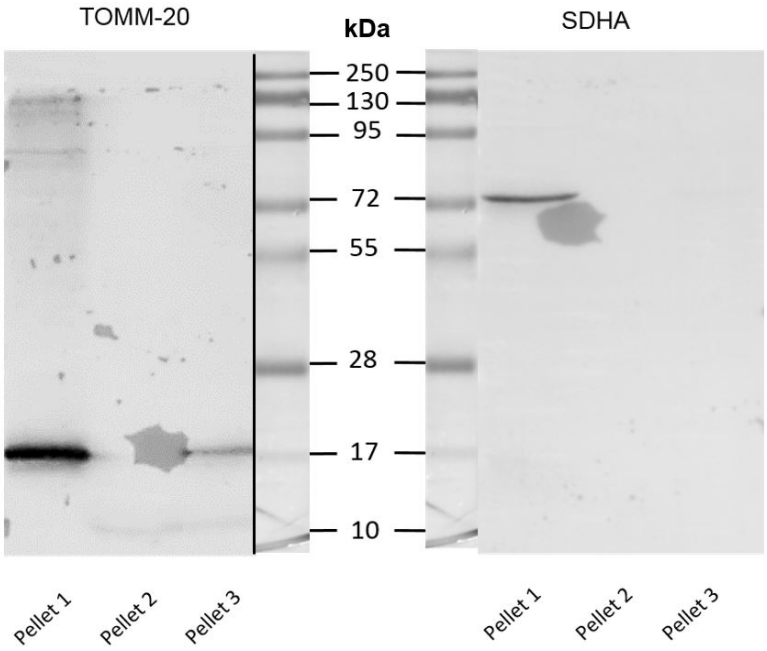

Figure 10. Representative immunoblot of TOMM-20 and SDHA in subcellular fractions from WT-HEK293 cells. Forty μg of protein samples from the subcellular fractions were processed as described in Materials and Methods and probed with anti-TOMM20 or anti-SDHA. The black vertical line indicates reprobing from the same gel.

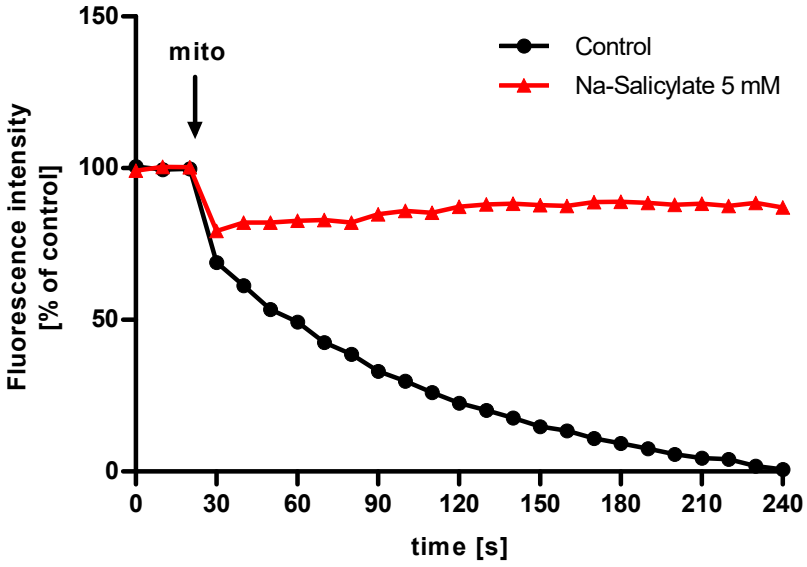

Figure 11. Time-course of R123 fluorescent signal in isolated mitochondria from WT-HEK293 cells. Mitochondria were resuspended in respiration buffer and mixed with 10 μM R123 solution in the presence or absence of Na-salicylate, and the fluorescence intensity at 538 nm was monitored. The black arrow indicates the time points at which mitochondria were added. Data are expressed as percentage of the fluorescent intensity before the mitochondria were added.

6.4 Energy state of mitochondria isolated from WT-HEK293 cells exposed to colistin

The impact of colistin exposure on the energy state of mitochondria was evaluated in WT-HEK293 cells after 48-hour incubation with colistin 500 µM or Na-Salicylate 5 mM. From the cells, mitochondria were extracted and protein content determined as previously described. Mitochondria at a final concentration of 0.25 mg/ml were exposed to a R123 10 µM solution and the fluorescence decay was monitored over time. Figure 12 shows that mitochondria from cells exposed to colistin displayed a reduced uptake of R123, suggesting a partial depolarization.

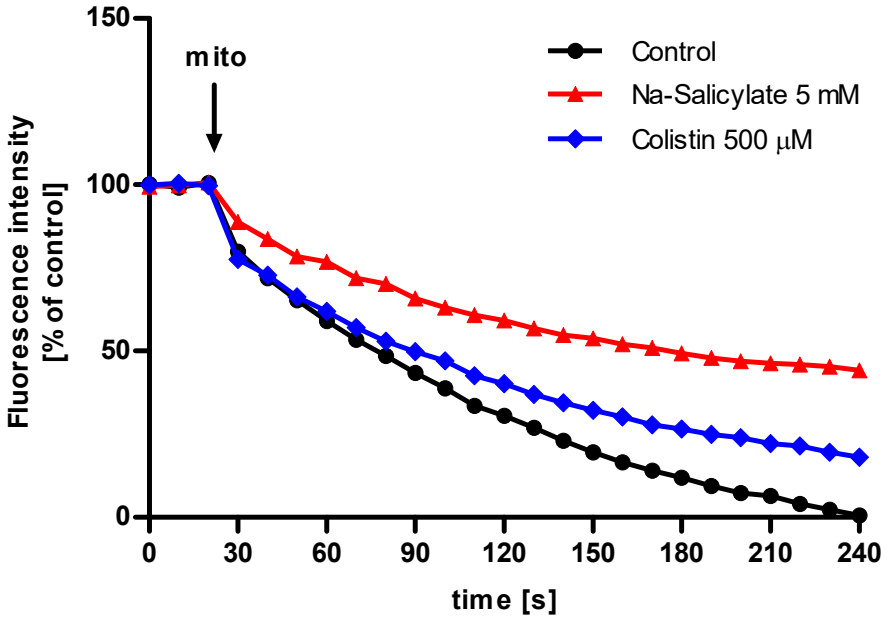

Figure 12. Time-course of R123 fluorescent signal in isolated mitochondria from WT-HEK293 cells. Isolated mitochondria were resuspended in respiration buffer and mixed with 10 µM R123 solution and the fluorescence intensity at 538 nm was monitored. The black arrow indicates the time points at which mitochondria were added. Data are expressed as percentage of the fluorescent intensity before the mitochondria were added.

6.5 Impact of colistin exposure on ATP production in WT-HEK293 cells

The main role of mitochondria is to generate ATP through oxidative phosphorylation. To assess the effect of colistin on intracellular ATP levels, WT-HEK-293 cells were exposed for 48 hours to the indicated concentrations of colistin, then the cells were lysed and the intracellular ATP levels were measured using Promega CellTiter-Glo® 2.0 Cell Viability Assay. Data were normalized for protein concentration. Figure 13

shows, that colistin exposure did not alter the intracellular levels of ATP. Notably, the treatment with oligomycin, a potent inhibitor of the H^+-ATP-Synthase, did not affect the intracellular levels of ATP significantly (P=0.24). Taken together the data suggest that WT-HEK293 cells did not rely on mitochondria-dependent ATP production.

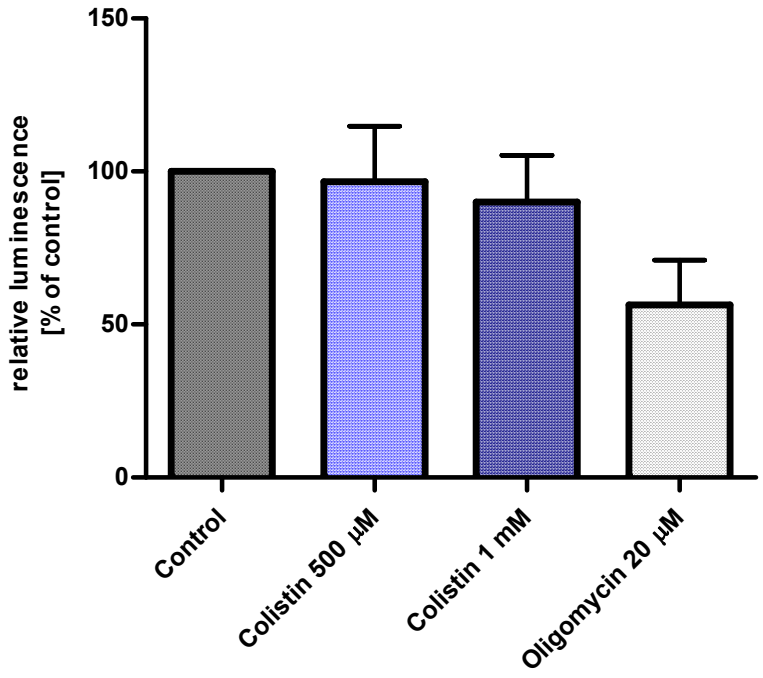

Figure 13. Measurement of intracellular ATP in WT-HEK293 cells treated with colistin. Cells were exposed for 48 hours to colistin at the indicated concentrations, then ATP levels were measured. Data are expressed as percentage of the luminescent intensity from untreated cells (control). Data represent the mean ± S.D. from three independent experiments.

6.6 Effect of colistin on isolated mitochondria from WT-HEK293 cells and from mouse kidney

To understand whether the mitochondrial dysfunction (Figure 8) was the primary effect of colistin exposure, or rather a consequence of other damaging events, R123 uptake by isolated mitochondria from WT-HEK293 cells was monitored in the presence or absence of colistin. In figure 15 it can be seen that colistin could induce a dose-dependent reduction of R123 accumulation (reduced quenching), suggesting a direct effect of colistin on mitochondrial membrane potential. Because mitochondria energy state can vary among tissues and cell types (Chance and Williams, 1955), we assessed the effect of colistin on mitochondria freshly extracted from mouse kidney. As observed in mitochondria extracted from WT-HEK293 cells, R123 uptake was reduced in presence of colistin, indicating membrane depolarization. In another setting

(Figure 16), mitochondria isolated from mouse kidney were incubated for 1 min with R123 solution then added with colistin (black arrow) to the indicated final concentrations. It can be seen that the colistin-induced mitochondrial dysfunction lead to a partial release of the intramitochondrial R123 as reflected by the enhanced fluorescent signal.

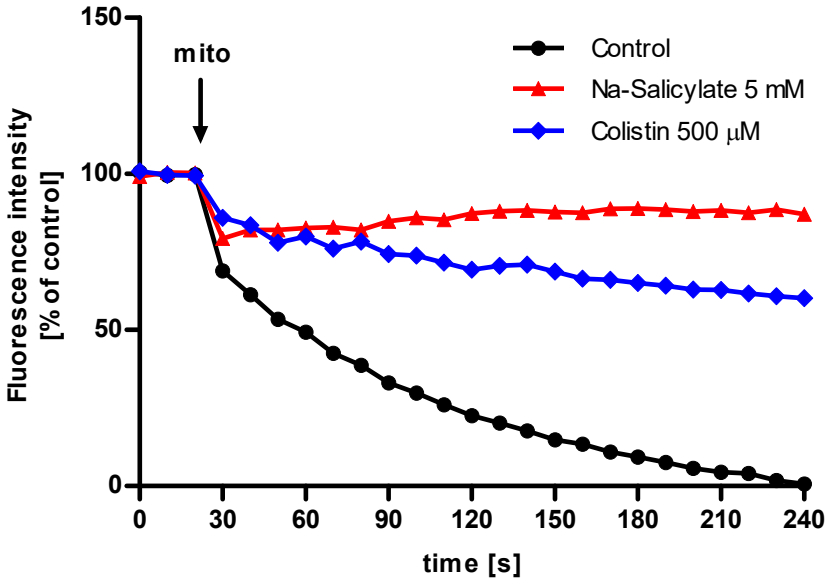

Figure 14. Time-course of R123 fluorescent signal in isolated mitochondria from WT-HEK293 cells. Mitochondria were resuspended in respiration buffer and mixed with 10 μM R123 solution and the fluorescence intensity at 538 nm was monitored. The black arrow indicates the time points at which mitochondria were added. Data are expressed as percentage of the fluorescent intensity before the mitochondria were added.

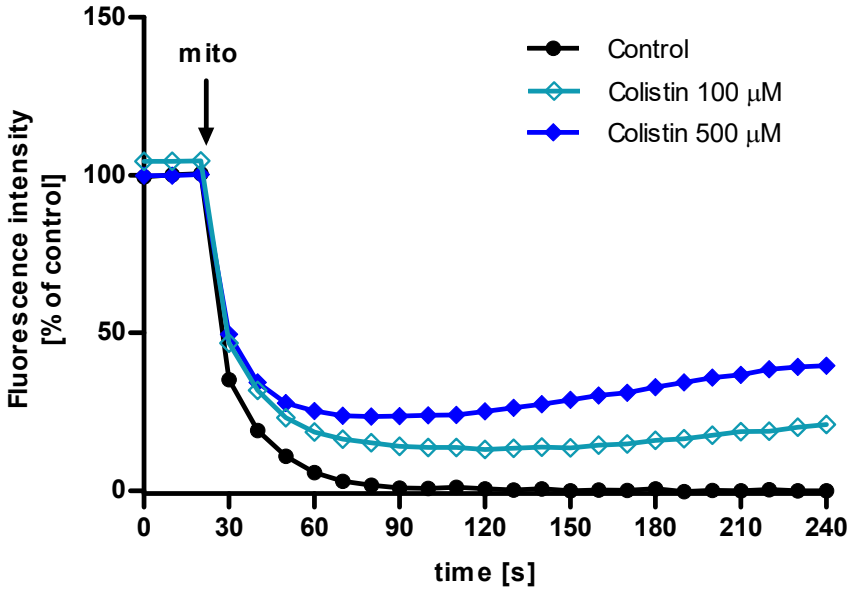

Figure 15. Time-course of R123 fluorescent signal in isolated mitochondria from mouse kidney. Mitochondria were resuspended in respiration buffer and mixed with 10 μM R123 solution and the fluorescence intensity at 538 nm was monitored. The black arrow indicates the time points at which mitochondria were added. Data are expressed as percentage of the fluorescent intensity before the mitochondria were added.

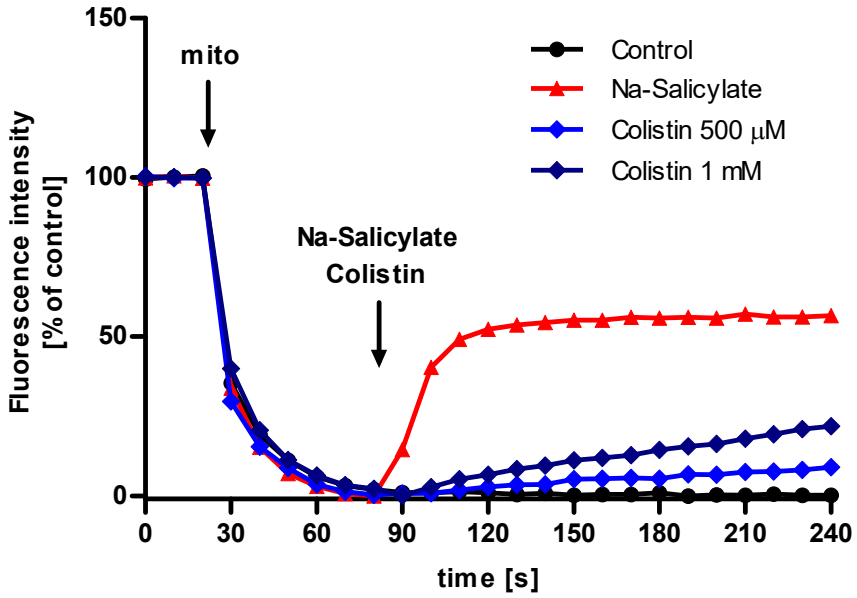

Figure 16. Time-course of R123 fluorescent signal in isolated mitochondria from mouse kidney. Mitochondria were resuspended in respiration buffer and mixed with 10 μM R123 solution and the fluorescence intensity at 538 nm was monitored. The black arrows indicate the time points at which mitochondria and the drugs were added. Data are expressed as percentage of the fluorescent intensity before the mitochondria were added.

6.7 Impact of other nephrotoxic antibiotics on isolated mitochondria from mouse kidney

Mitochondrial toxicity has been proposed also for other recognized nephrotoxic antibiotics as aminoglycosides (Davey et al., 1970) and vancomycin (Arimura et al., 2012). We assessed the impact of gentamycin (a member of the aminoglycoside family) and vancomycin on mitochondrial membrane potential in comparison with colistin. Figure 17 shows the effect of gentamycin 1 mM and vancomycin 1 mM in comparison with colistin 1 mM on the R123 uptake of isolated mitochondria from mouse kidney cells. The effect of the former two showed to be less pronounced. This indicates that vancomycin and gentamycin interfere with the mitochondrial membrane potential to a lesser extent. This comparison also further accentuates the depolarizing effect of colistin on the mitochondrial membrane and underlines the probability of involvement of mitochondria in its toxicity.

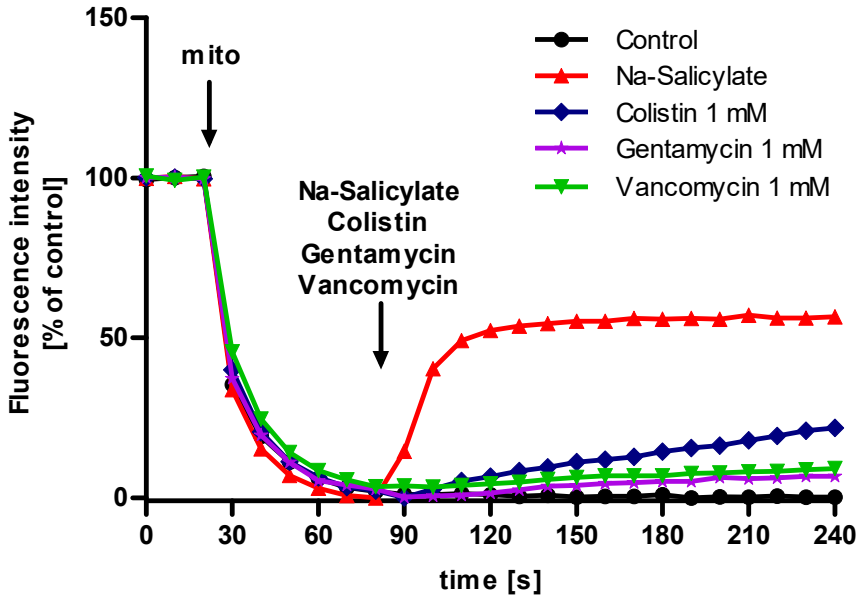

Figure 17. Time-course of R123 fluorescent signal in isolated mitochondria from mouse kidney. Isolated mitochondria from mouse kidney tissue were resuspended in respiration buffer and mixed with 10 μM R123 solution and the fluorescence intensity at 538 nm was monitored. The black arrows indicate the time points at which mitochondria and the different drugs were added. Data are expressed as percentage of the fluorescent intensity before the mitochondria were added.

6.8 Effect of co-incubation of inhibitors of the MPTP

The main sensor of mitochondrial function is the mitochondrial permeability transition pore (MPTP) (Lemasters et al., 1998). The opening of the MPTP can be a cause or a consequence of the membrane potential depolarization. To understand whether colistin-induced depolarization was dependent on the MPTP opening we reviewed the literature for documented MPTP opening inhibitors. We found very well-characterized inhibitors such as ADP (Sokolova et al., 2013) and cyclosporine A; other reports suggested that L-carnitine and fatty acid-free bovine serum albumin (BSA) could also inhibit the opening of the pore (Li et al., 2015; Hurst et al., 2016). We tested the effect of these compounds on colistin-induced depolarization.

Figure 18 shows that mitochondria co-incubated with ADP were not sensitive to colistin. The other MPTP inhibitors cyclosporin A, L-carnitine and BSA failed to protect from membrane depolarization.

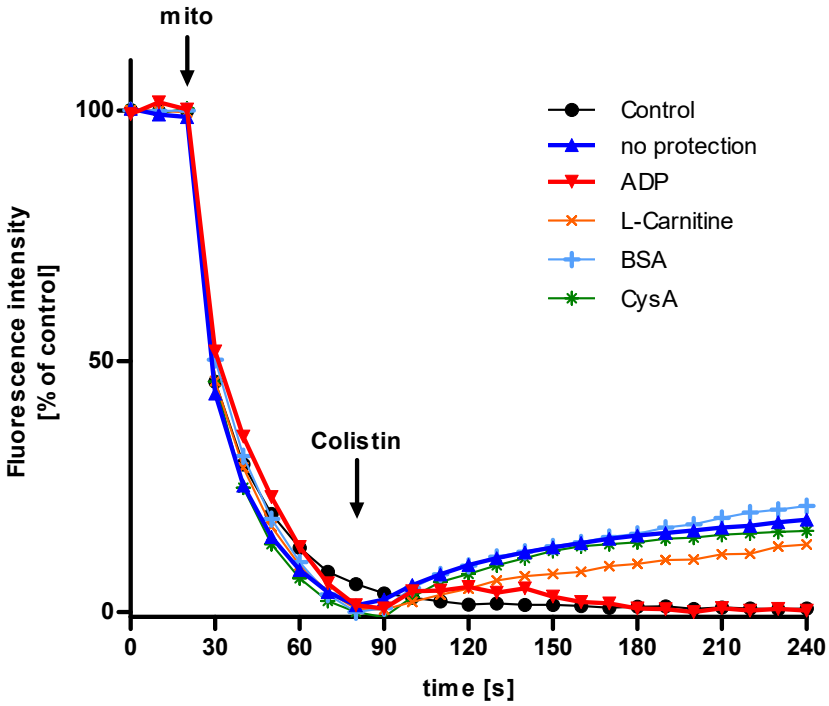

Figure 18. Time-course of the R123 fluorescent signal in isolated mitochondria from mouse kidney. Isolated mitochondria from mouse kidney were resuspended in respiration buffer and mixed with 10 μM R123 solution and the fluorescence intensity at 538 nm was monitored. The black arrows indicate the time points at which mitochondria and colistin were added. Data are expressed as percentage of the fluorescent intensity before the mitochondria were added.

6.9 Mitochondrial swelling experiment with WT-HEK293 cells

MPTP opening induces mitochondrial swelling. To assess the effect of colistin on mitochondrial volume, isolated mitochondria were resuspended in swelling buffer, then exposed to colistin and the optical absorbance at 560 nm was monitored. Swelling of mitochondria is accompanied by a reduced light scattering (decreased absorbance), vice versa, shrinking of mitochondria is reflected by an increased absorbance. Isolated mitochondria were diluted at a final concentration of 0.25 mg/mL in swelling buffer containing the indicated solutions. Absorption was monitored at 560 nm and is shown in Figure 19. $CaCl_2$ was used as positive control for mitochondrial swelling. Mitochondria exposed to $CaCl_2$ at the extracellular concentration of 500 μM showed ~ 20% decrease in absorption ($P<0.05$) as a result of solutes and water influx through the open MPTP. Polyethylene glycol 3000 (PEG-3000) should induce water efflux by exerting an oncotic pressure against the mitochondrial outer membrane and, in turn, shrinking of the mitochondria. It can be seen that mitochondria exposed to PEG-3000 displayed a slightly higher (5%) light scattering as compared tothe control. Mitochondria exposed to colistin showed significant increase in absorption in a dose-dependent manner with a mean increase of approx. 22% ($P<0.001$) and 32% ($P<0.0001$) respectively. This strongly suggests significant shrinking of mitochondria exposed to colistin in a concentration dependent manner.

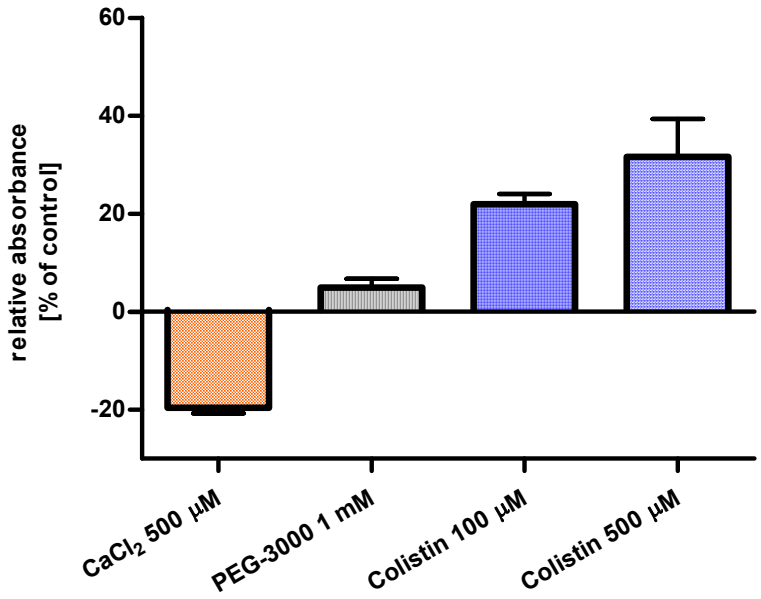

Figure 19. Assessment of mitochondrial morphology after exposure to colistin. Isolated mitochondria were transferred to 96-well plates and different treatments applied. Absorption was measured at 562 nm. Data are expressed as percentage of the absorption intensity relative to the untreated control and as mean ± S.D. Multiple analysis was performed by one-way ANOVA test. Dunnett test was used for Post Hoc.

7 Discussion

The proposed model of colistin induced-nephrotoxicity is based on electrostatic interaction of its cationic structure and the interference of its D-amino acid content as well as the fatty acid component with the eukaryotic cellular membrane. A possible result isthe influx of cations, anions and water, with subsequent cell swelling and lysis (Falagas and Kasiakou, 2006). Such a mechanism assumes that mammalian and bacterial cell membranes are similar. However, the biochemical composition of eukaryotic cell membranes differs substantially from that of bacteria. Gram-negative bacteria outer cell membranes contain a significant amount of negatively charged lipids (phosphatidylglycerol and cardiolipins) whereas eukaryotic cell membranes are enriched in cholesterol and their outer layer is essentially neutral. These differences in net charge and lipid contents make electrostatic interference with, and insertion into, mammalian membranes of colistin, a five-fold positively charged cationic polypeptide, unlikely. Consistently, no obvious hemolytic events were observed when mammalian erythrocytes were exposed to cationic polypeptides (Glukhov et al., 2005). On the other hand, gram-negative bacteria membranes are evolutionary close to the mitochondrial membranes, making the interaction with colistin more likely. We demonstrated that mitochondria of WT-HEK293 cells were completely depolarized upon colistin exposure. Despite the dramatic effect at the membrane potential level, we did not appreciate any macroscopic change in TOMM-20 staining in cells treated with colistin, suggesting that membrane depolarization was an early event in colistin-induced mitochondrial toxicity. Furthermore, higher level of intracellular L-carnitine, an important co-factor in mitochondria energy state, could protect WT-HEK293 cells from colistin-induced mitochondrial damage.

The membrane potential across the inner membrane of mitochondria is ~ 220-240 mV and consists of the mitochondrial membrane potential ($\Delta\psi$, a charge or electrical gradient) and the mitochondrial pH gradient (ΔpH, an H^+ chemical or concentration gradient) (Mitchell and Moyle, 1969). The net accumulation of H^+ outside the inner membrane then flows back into the mitochondria through the ATP-generating F1/F0 ATP-synthase, thus producing ATP from ADP + Pi. Hence, the mitochondrial membrane depolarization would result in a rapid drop of the cellular ATP levels. The ATP content from WT-HEK293 cells exposed to colistin for 48 hours was similar to that of untreated cells, in apparent contradiction with the marked membrane depolarization observed in similar experimental conditions. The possible explanation for this conflicting data might lie in a metabolic switch often observed in culture cells. Cell lines

are metabolically adapted for rapid growth under hypoxic and acidic conditions, and they derive almost all of their energy from glycolysis rather than via mitochondrial oxidative phosphorylation (OXPHOS), despite the presence of competent mitochondria. Such adaption is known as Crabtree effect (Crabtree, 1929). In such cells, mitochondrial toxins have little effect on cell growth or viability (Marroquin et al., 2007). In line with this, oligomycin is a potent inhibitor of the F0 subunit of H^+-ATP-synthase but failed to lower cellular ATP contents of exposed WT-HEK293 cells. The Crabtree effect can be by-passed by growing the cells in a galactose growth medium: galactose-derived glycolysis yields no net ATP, forcing the cells to rely on mitochondrial ATP production (Marroquin et al., 2007). The potency of oligomycin to deplete the intracellular level of ATP production increases by 5 orders of magnitude in a galactose growth medium (IC_{50}gal=3 nM, IC_{50}glu=300 μM) (Swiss et al., 2013).

The membrane depolarization induced by colistin might begin with an alteration of the membrane permeability via mechanical damage to the outer mitochondrial membrane (OMM), which resembles the lipid composition of gram-negative cells. A number of studies have shown that polymyxins induce a concentration dependent transition in mitochondrial morphology from filamentous to fragmented shape, which was interpreted as a sign of stress (Azad et al., 2015). Damage to mitochondrial ultrastructure and alteration of expressed enzymes after exposure of neuronal cells to clinical doses of colistin have also been observed (Dai et al., 2013a). It seems unlikely that a solely increased OMM-permeability can induce membrane depolarization. It has been reported that permeabilized mitochondria can sustain the membrane potential and the mitochondrial function through the release of cytochrome c (Waterhouse et al., 2001). More likely, the increased OMM-permeability could ease the access of colistin to the intramembranous space that might otherwise be difficult in consideration of the cationic nature of colistin.

Colistin might also induce the opening of the mitochondrial permeability transition pore (MPTP). The MPTP is a mitochondria-specific protein complex spanning the outer and the inner membranes. A permanent opening of this pore allows molecules of up to a size of 1’500 Dalton to pass freely through the outer and inner membrane with dramatic changes in mitochondrial homoeostasis and result in dissipation of the proton gradient, depolarization and induction of apoptotic or necrotic signals. The main factor for MPTP opening is the raise of the Ca^{++} concentration in the matrix (Hurst et al., 2016). One hypothesis is that the mitochondrial shrinkage induced by colistin might raise the concentration of Ca^{++} in the matrix, which, in turn, would induce the opening of the

pore. An increased mitochondrial permeability in mitochondria from kidney of mice exposed to colistin has been reported (Dai et al., 2014). In our setting colistin-induced depolarization of the mitochondrial membrane was completely abolished when isolated mitochondria were co-incubated with ADP, a known inhibitor of the MPTP (Sokolova et al., 2013). When cyclosporine A was used to inhibit the opening of the pore, no protection was observed. This is consistent with previous work which demonstrated that cyclosporine A's inhibitory effect was reduced in shrunken mitochondria (Hurst et al., 2016). Interestingly, L-carnitine, which was also reported to inhibit the opening of the pore (Virmani et al., 2003) did not protect the isolated mitochondria from colistin-induced depolarization. L-carnitine may still protect the cells by inhibiting the opening of the MPTP, but in an indirect fashion.

The mitochondrial stress induced by colistin has already been reported both in vitro (Dai et al., 2013b) and in vivo (Dai et al., 2014). None of these studies could define whether colistin directly interacted with mitochondria, thus representing a primary event in colistin-induced damage, or if the observed long-term damage was just part of the apoptotic or necrotic machinery. To the best of our knowledge, this is the first evidence that colistin directly interacts with mitochondria inducing a rapid depolarization of the mitochondrial membrane potential within seconds. Mitochondrial depolarizing agents can be classified as uncouplers and inhibitors. Typical uncouplers are carbonyl cyanide-4-(trifluoromethoxy)phenylhydrazone (FCCP), carbonyl cyanide m-chlorophenyl hydrazone (CCCP), Na-salicylate and free fatty acids. Such molecules are usually weak anions that act as ionophores and bring H^+ across the mitochondrial membranes, dissipating the proton gradient. The presence of a short fatty acid chain might confer some uncoupling properties to colistin (Broekemeier and Pfeiffer, 1995; Di Paola and Lorusso, 2006). However, considering the whole peptide colistin is highly cationic in nature, the possibility of it acting as an uncoupler may be limited.

The membrane potential across the inner membrane is generated as oxidized substrates (e.g. pyruvate, succinate) release electrons to cofactors such as NADH or $FADH_2$. These electrons are passed through electron carriers in respiratory chain complexes with increasing oxidation potentials, ultimately reducing molecular oxygen to water. If one of this complex is inhibited the electrochemical gradient across the inner membrane cannot be sustained resulting in membrane depolarization. Many drugs (including antibiotics) and toxins have been shown to induce mitochondrial stress by inhibiting the electron transport chain. Amytal, a barbiturate, blocks the electron transfer between NADH dehydrogenase and coenzyme Q and therefore

inhibits complex I (Ernster, 1963). Lonidamin, an anticancer agent inhibits the succinate-ubiquinone reductase activity of complex II (Guo et al., 2016). Antimycin A, an antibiotic produced by Streptomyces griseous that is used as a piscicide, inhibits complex III of the electron transport chain by binding to its bc_1 segment (Berden and Slater, 1972). Potassium cyanide (KCN) inhibits complex IV of the respiratory chain by binding to the Fe^{+++} in the hem-group of cytochrome C (Jensen et al., 1984). In our experimental setting, succinate was employed as substrate. Because succinate is a substrate for complex II, it is unlikely that the colistin-induced depolarization is due to an interaction at the level of complex I. Inhibition of complex II, III and IV by colistin cannot be ruled out. While complex I-IV contribute to the generation of the membrane potential, the H^+-ATP-synthase dissipates the potential by using the protons accumulated at the interspace to generate ATP. The inhibition of the H^+-ATP-synthase with the antibiotic oligomycin, in presence of a function electron transport, increases the membrane potential (hyperpolarization) (Perry et al., 2011). Our data indicates that an interaction between colistin and the H^+-ATP-synthase is unlikely.

Protecting mitochondria with L-carnitine from colistin is an intriguing strategy to implement colistin pharmacology. The average plasma concentration of L-carnitine is ~ 15-50 μM, depending on age and gender among other factors (Vaz and Wanders, 2002). L-carnitine is mainly reabsorbed in the tubules by OCTN2 with an influx K_m of ~ 5 μM, indicating that under physiological conditions OCTN2 is nearly saturated and L-carnitine supplementation would fail to increase its intracellular levels. Children lacking a functioning OCTN2 are affected by primary systemic carnitine deficiency (SCD; OMIM 212140) (Nezu et al., 1999). However oral L-carnitine supplementation can sustain normal plasma levels of L-carnitine in these patients, suggesting that, at supraphysiological levels, other carriers (e.g. OCTN1) could mediate L-carnitine reabsorption. Intravenous administration of L-carnitine could reach a plasma peak of 200 μM and effectively raise its intracellular levels possibly to the point of protection from colistin damage (Rasmussen et al., 2015).

8 References

Apell H-JK, H.; Schmitt, B. (2004) Reviews of Physiology, Biochemistry and Pharmacology 150 (Nilius B, Gudermann, Th., Jahn, R., Lill, R., Petersen, O.H., de Tombe, P.P. ed, Springer.

Arimura Y, Yano T, Hirano M, Sakamoto Y, Egashira N, and Oishi R (2012) Mitochondrial superoxide production contributes to vancomycin-induced renal tubular cell apoptosis. *Free Radic Biol Med* 52:1865-1873.

Averill BA (2012) Figure 18.20, The ATP Cycle. *Principles of General Chemistry* Thermodynamis and Life.

Azad MA, Akter J, Rogers KL, Nation RL, Velkov T, and Li J (2015) Major pathways of polymyxin-induced apoptosis in rat kidney proximal tubular cells. *Antimicrob Agents Chemother* 59:2136-2143.

Baker H, DeAngelis B, and Frank O (1988) Vitamins and other metabolites in various sera commonly used for cell culturing. *Experientia* 44:1007-1010.

Barza M and Weinstein L (1976) Pharmacokinetics of the penicillins in man. *Clin Pharmacokinet* 1:297-308.

Berden JA and Slater EC (1972) The allosteric binding of antimycin to cytochrome b in the mitochondrial membrane. *Biochim Biophys Acta* 256:199-215.

Berg J.M., Tymoczko J.L., Gatto jr. G.J., Stryer L. (2018) Die oxidative Phosphorylierung. In: Stryer Biochemie. Springer Spektrum, Berlin, Heidelberg

Bergogne-Berezin E and Towner KJ (1996) Acinetobacter spp. as nosocomial pathogens: microbiological, clinical, and epidemiological features. *Clin Microbiol Rev* 9:148-165.

Bertram G. Katzung M, PhD; Anthony J. Trevor, PhD; Marieke Kruidering-Hall, PhD (2015) Katzung & Trevor's Pharmacology: Examination & Board Review, 11e.

Broekemeier KM and Pfeiffer DR (1995) Inhibition of the mitochondrial permeability transition by cyclosporin A during long time frame experiments: relationship between pore opening and the activity of mitochondrial phospholipases. *Biochemistry* 34:16440-16449.

Chance B and Williams GR (1955) Respiratory enzymes in oxidative phosphorylation. IV. The respiratory chain. *J Biol Chem* 217:429-438.

Chen LB (1988) Mitochondrial membrane potential in living cells. *Annu Rev Cell Biol* 4:155-181.

Christ W (1991) Pharmacological properties of cephalosporins. *Infection* 19 Suppl 5:S244-252.

Chukwudi CU (2016) rRNA Binding Sites and the Molecular Mechanism of Action of the Tetracyclines. *Antimicrob Agents Chemother* 60:4433-4441.

Crabtree HG (1929) Observations on the carbohydrate metabolism of tumours. *Biochem J* 23:536-545.

Craig WA (1998) Pharmacokinetic/pharmacodynamic parameters: rationale for antibacterial dosing of mice and men. *Clinical infectious diseases : an official publication of the Infectious Diseases Society of America* 26:1-10; quiz 11-12.

Dai C, Li J, and Li J (2013a) New insight in colistin induced neurotoxicity with the mitochondrial dysfunction in mice central nervous tissues. *Exp Toxicol Pathol* 65:941-948.

Dai C, Li J, Tang S, Li J, and Xiao X (2014) Colistin-induced nephrotoxicity in mice involves the mitochondrial, death receptor, and endoplasmic reticulum pathways. *Antimicrob Agents Chemother* 58:4075-4085.

Dai C, Zhang D, Li J, and Li J (2013b) Effect of colistin exposure on calcium homeostasis and mitochondria functions in chick cortex neurons. *Toxicol Mech Methods* 23:281-288.

Davey PJ, Haslam JM, and Linnane AW (1970) Biogenesis of mitochondria. 12. The effects of aminoglycoside antibiotics on the mitochondrial and cytoplasmic protein-synthesizing systems of Saccharomyces cerevisiae. *Arch Biochem Biophys* 136:54-64.

Denning K (2007) Introduction to Archaeology and Palaeoanthropology: Humanity's Journeys.

Di Paola M and Lorusso M (2006) Interaction of free fatty acids with mitochondria: coupling, uncoupling and permeability transition. *Biochim Biophys Acta* 1757:1330-1337.

Emaus RK, Grunwald R, and Lemasters JJ (1986) Rhodamine 123 as a probe of transmembrane potential in isolated rat-liver mitochondria: spectral and metabolic properties. *Biochim Biophys Acta* 850:436-448.

Ernster L, Dallner, G., Azzone, G. F., (1963) Differential Effects of Rotenone and Amytal on Mitochondrial Electron and Energy Transfer. *The Journal of Biological Chemistry* 238.

Falagas ME and Kasiakou SK (2005) Colistin: the revival of polymyxins for the management of multidrug-resistant gram-negative bacterial infections. *Clin Infect Dis* 40:1333-1341.

Falagas ME and Kasiakou SK (2006) Toxicity of polymyxins: a systematic review of the evidence from old and recent studies. *Crit Care* 10:R27.

Freeman WHaC (2008) Figure 12-8, Molecular Cell Biology, Sixth Edition, pp The citric acid cycle.

Freissmuth M. (2016) Antibakterielle Chemotherapie. In: Pharmakologie und Toxikologie. Springer-Lehrbuch. Springer, Berlin, Heidelberg

Frezza C, Cipolat S, and Scorrano L (2007) Organelle isolation: functional mitochondria from mouse liver, muscle and cultured fibroblasts. *Nat Protoc* 2:287-295.

Gai Z, Visentin M, Hiller C, Krajnc E, Li T, Zhen J, and Kullak-Ublick GA (2016) Organic Cation Transporter 2 Overexpression May Confer an Increased Risk of Gentamicin-Induced Nephrotoxicity. *Antimicrob Agents Chemother* 60:5573-5580.

Glukhov E, Stark M, Burrows LL, and Deber CM (2005) Basis for selectivity of cationic antimicrobial peptides for bacterial versus mammalian membranes. *J Biol Chem* 280:33960-33967.

Guo L, Shestov AA, Worth AJ, Nath K, Nelson DS, Leeper DB, Glickson JD, and Blair IA (2016) Inhibition of Mitochondrial Complex II by the Anticancer Agent Lonidamine. *J Biol Chem* 291:42-57.

Halestrap AP (2010) A pore way to die: the role of mitochondria in reperfusion injury and cardioprotection. *Biochemical Society transactions* 38:841-860.

Heidrich HG, Stahn R, and Hannig K (1970) The surface charge of rat liver mitochondria and their membranes. Clarification of some controversies concerning mitochondrial structure. *J Cell Biol* 46:137-150.

Hurst S, Hoek J, and Sheu SS (2016) Mitochondrial Ca2+ and regulation of the permeability transition pore. *J Bioenerg Biomembr*.

Jensen P, Wilson MT, Aasa R, and Malmstrom BG (1984) Cyanide inhibition of cytochrome c oxidase. A rapid-freeze e.p.r. investigation. *Biochem J* 224:829-837.

Jonckheere AI, Smeitink JA, and Rodenburg RJ (2012) Mitochondrial ATP synthase: architecture, function and pathology. *J Inherit Metab Dis* 35:211-225.

Kapoor G, Saigal S, and Elongavan A (2017) Action and resistance mechanisms of antibiotics: A guide for clinicians. *J Anaesthesiol Clin Pharmacol* 33:300-305.

Kassamali Z, Jain R, and Danziger LH (2015) An update on the arsenal for multidrug-resistant Acinetobacter infections: polymyxin antibiotics. *Int J Infect Dis* 30:125-132.

Koch-Weser J, Sidel VW, Federman EB, Kanarek P, Finer DC, and Eaton AE (1970) Adverse effects of sodium colistimethate. Manifestations and specific reaction rates during 317 courses of therapy. *Ann Intern Med* 72:857-868.

Koomanachai P, Tiengrim S, Kiratisin P, and Thamlikitkul V (2007) Efficacy and safety of colistin (colistimethate sodium) for therapy of infections caused by multidrug-resistant Pseudomonas aeruginosa and Acinetobacter baumannii in Siriraj Hospital, Bangkok, Thailand. *Int J Infect Dis* 11:402-406.

Kumazawa J and Yagisawa M (2002) The history of antibiotics: the Japanese story. *J Infect Chemother* 8:125-133.

Kwiatkowska B and Maslinska M (2012) Macrolide therapy in chronic inflammatory diseases. *Mediators Inflamm* 2012:636157.

Lemasters JJ, Nieminen AL, Qian T, Trost LC, Elmore SP, Nishimura Y, Crowe RA, Cascio WE, Bradham CA, Brenner DA, and Herman B (1998) The mitochondrial permeability transition in cell death: a common mechanism in necrosis, apoptosis and autophagy. *Biochim Biophys Acta* 1366:177-196.

Levison ME and Levison JH (2009) Pharmacokinetics and pharmacodynamics of antibacterial agents. *Infect Dis Clin North Am* 23:791-815, vii.

Li J, Milne RW, Nation RL, Turnidge JD, Smeaton TC, and Coulthard K (2003) Use of high-performance liquid chromatography to study the pharmacokinetics of colistin sulfate in rats following intravenous administration. *Antimicrobial agents and chemotherapy* 47:1766-1770.

Li S, Guo J, Ying Z, Chen S, Yang L, Chen K, Long Q, Qin D, Pei D, and Liu X (2015) Valproic acid-induced hepatotoxicity in Alpers syndrome is associated with mitochondrial permeability transition pore opening-dependent apoptotic sensitivity in an induced pluripotent stem cell model. *Hepatology* 61:1730-1739.

Lopez-Novoa JM, Quiros Y, Vicente L, Morales AI, and Lopez-Hernandez FJ (2011) New insights into the mechanism of aminoglycoside nephrotoxicity: an integrative point of view. *Kidney Int* 79:33-45.

Lu X, Chan T, Xu C, Zhu L, Zhou QT, Roberts KD, Chan HK, Li J, and Zhou F (2016) Human oligopeptide transporter 2 (PEPT2) mediates cellular uptake of polymyxins. *The Journal of antimicrobial chemotherapy* 71:403-412.

Ma Z, Wang J, Nation RL, Li J, Turnidge JD, Coulthard K, and Milne RW (2009) Renal disposition of colistin in the isolated perfused rat kidney. *Antimicrobial agents and chemotherapy* 53:2857-2864.

Margulis L (1975) Symbiotic theory of the origin of eukaryotic organelles; criteria for proof. *Symp Soc Exp Biol*:21-38.

Marroquin LD, Hynes J, Dykens JA, Jamieson JD, and Will Y (2007) Circumventing the crabtree effect: Replacing media glucose with galactose increases susceptibility of HepG2 cells to mitochondrial toxicants. *Toxicological Sciences* 97:539-547.

Michael CA, Dominey-Howes D, and Labbate M (2014) The antimicrobial resistance crisis: causes, consequences, and management. *Front Public Health* 2:145.

Mihaylova MM, Shaw RJ. The AMP-activated protein kinase (AMPK) signaling pathway coordinates cell growth, autophagy, & metabolism. *Nature cell biology*. 2011;13(9):1016-1023.

Milane L, Trivedi M, Singh A, Talekar M, and Amiji M (2015) Mitochondrial biology, targets, and drug delivery. *J Control Release* 207:40-58.

Mitchell P and Moyle J (1969) Estimation of membrane potential and pH difference across the cristae membrane of rat liver mitochondria. *Eur J Biochem* 7:471-484.

Mohamed YF, Abou-Shleib HM, Khalil AM, El-Guink NM, and El-Nakeeb MA (2016) Membrane permeabilization of colistin toward pan-drug resistant Gram-negative isolates. *Braz J Microbiol* 47:381-388.

Nezu J, Tamai I, Oku A, Okashi R, Yabuuchi H, Hashimoto N, Nikaido H, Sai Y, Koizumi A, Shoji Y, Takada G, Matsuishi T, Yoshino M, Kato H, Ohura T, Tsujimoto G, Hayakawa J, Shimane M, Tsuji A (1999) Primary systemic carnitine deficiency is caused mutations in a gene encoding sodium ion-dependent carnitine transporter. *Nat Genet 21 91-4*

Nikaido H (2009) Multidrug resistance in bacteria. *Annu Rev Biochem* 78:119-146.

Nilsson A, Goodwin RJA, Swales JG, Gallagher R, Shankaran H, Sathe A, Pradeepan S, Xue AX, Keirstead N, Sasaki JC, Andren PE, and Gupta A (2015) Investigating Nephrotoxicity of Polymyxin Derivatives by Mapping Renal Distribution Using Mass Spectrometry Imaging. *Chem Res Toxicol* 28:1823-1830.

Packer L (1960) Metabolic and structural states of mitochondria. I. Regulation by adenosine diphosphate. *J Biol Chem* 235:242-249.

Pazhayattil GS and Shirali AC (2014) Drug-induced impairment of renal function. *Int J Nephrol Renovasc Dis* 7:457-468.

Periti P, Mazzei T, Mini E, and Novelli A (1989) Clinical pharmacokinetic properties of the macrolide antibiotics. Effects of age and various pathophysiological states (Part II). *Clin Pharmacokinet* 16:261-282.

Perry SW, Norman JP, Barbieri J, Brown EB, and Gelbard HA (2011) Mitochondrial membrane potential probes and the proton gradient: a practical usage guide. *Biotechniques* 50:98-115.

Pogue JM, Ortwine JK, and Kaye KS (2015) Optimal Usage of Colistin: Are We Any Closer? *Clinical infectious diseases : an official publication of the Infectious Diseases Society of America* 61:1778-1780.

Rasmussen J, Thomsen JA, Olesen JH, Lund TM, Mohr M, Clementsen J, Nielsen OW, and Lund AM (2015) Carnitine levels in skeletal muscle, blood, and urine in patients with primary carnitine deficiency during intermission of L-carnitine supplementation. *JIMD Rep* 20:103-111.

Rasola A and Bernardi P (2011) Mitochondrial permeability transition in Ca(2+)-dependent apoptosis and necrosis. *Cell Calcium* 50:222-233.

Rothstein DM (2016) Rifamycins, Alone and in Combination.*Cold Spring Harb Persp Med* 6

Smith BJ (1994) SDS polyacrylamide gel electrophoresis of proteins. *Methods Mol Biol* 32:23-34.

Smith MJ and Moses V (1960) Uncoupling reagents and metabolism. 1. Effects of salicylate and 2:4-dinitrophenol on the incorporation of C from labelled glucose and acetate into the soluble intermediates of isolated rat tissues. *Biochem J* 76:579-585.

Smith PK, Krohn RI, Hermanson GT, Mallia AK, Gartner FH, Provenzano MD, Fujimoto EK, Goeke NM, Olson BJ, and Klenk DC (1985) Measurement of protein using bicinchoninic acid. *Anal Biochem* 150:76-85.

Sokolova N, Pan S, Provazza S, Beutner G, Vendelin M, Birkedal R, and Sheu SS (2013) ADP protects cardiac mitochondria under severe oxidative stress. *PLoS One* 8:e83214.

Swiss R, Niles A, Cali JJ, Nadanaciva S, and Will Y (2013) Validation of a HTS-amenable assay to detect drug-induced mitochondrial toxicity in the absence and presence of cell death. *Toxicol In Vitro* 27:1789-1797.

Vaz FM and Wanders RJA (2002) Carnitine biosynthesis in mammals. *Biochemical Journal* 361:417-429.

Ventola CL (2015) The antibiotic resistance crisis: part 1: causes and threats. *PT*40:277-283.

Virmani A, Gaetani F, Imam S, Binienda Z, and Ali S (2003) Possible mechanism for the neuroprotective effects of L-carnitine on methamphetamine-evoked neurotoxicity. *Ann N Y Acad Sci* 993:197-207; discussion 287-198.

Visentin M, Gai Z, Torozi A, Hiller C, and Kullak-Ublick GA (2017) Colistin is substrate of the carnitine/organic cation transporter 2 (OCTN2, SLC22A5). *Drug Metab Dispos* 45:1240-1244.

Waterhouse NJ, Goldstein JC, von Ahsen O, Schuler M, Newmeyer DD, and Green DR (2001) Cytochrome c maintains mitochondrial transmembrane potential and ATP generation after outer mitochondrial membrane permeabilization during the apoptotic process. *J Cell Biol* 153:319-328.

WHO (2015) WHO Model Lists of Essential Medicines.

Yabuuchi H, Tamai I, Nezu J, Sakamoto K, Oku A, Shimane M, Sai Y, and Tsuji A (1999) Novel membrane transporter OCTN1 mediates multispecific, bidirectional, and pH-dependent transport of organic cations. *The Journal of pharmacology and experimental therapeutics* 289:768-773.

Yun B, Azad MA, Wang J, Nation RL, Thompson PE, Roberts KD, Velkov T, and Li J (2015) Imaging the distribution of polymyxins in the kidney. *The Journal of antimicrobial chemotherapy* 70:827-829.

Zavascki AP, Goldani LZ, Li J, and Nation RL (2007) Polymyxin B for the treatment of multidrug-resistant pathogens: a critical review. *J Antimicrob Chemother* 60:1206-1215.

9 Acknowledgments

I am grateful to my main supervisor, Prof. Gerd Kullak-Ublick, for giving me the opportunity to gain an insight into the world of pharmalogical research and work in his lab. I am very thankful to my direct supervisor, PhD Michele Visentin, for guiding my experimental work, supporting me in writing and always patiently answering my questions with the best of his knowledge.

Thank you, Dr. Gai Zhibo, for the opportunity to work with a confocal microscope and your guidance through the respective experiments. Great thanks also to Christian Hiller for teaching me good microbiological practice and his technical help in various experiments.

I am also thankful to my fellow colleagues Evelin Krajnc, Julia Steiger and Stephanie for all the good laughs and company during my time in the laboratory of the Department of Clinical Pharmacology and Toxicology in Schlieren.

I am especially grateful to my parents, Doris and Hubert Gantenbein. Thank you for all your support and effort towards me over the years of my studying and during my dissertation.

10 Bestätigung der Eigenleistung

Dissertation

Ich erkläre ausdrücklich, dass es sich bei der von mir im Rahmen des Studiengangs

Humanmedizin

eingereichten schriftlichen Arbeit mit dem Titel

Cellular and molecular mechanisms of colistin-induced nephrotoxicity

um eine von mir selbst und ohne unerlaubte Beihilfe sowie *in eigenen Worten* verfasste Dissertation handelt.

Ich bestätige überdies, dass die Arbeit als Ganzes oder in Teilen weder bereits einmal zur Abgeltung anderer Studienleistungen an der Universität Zürich oder an einer anderen Universität oder Ausbildungseinrichtung eingereicht worden ist.

Verwendung von Quellen

Ich erkläre ausdrücklich, dass ich *sämtliche* in der oben genannten Arbeit enthaltenen Bezüge auf fremde Quellen (einschliesslich Tabellen, Grafiken u. Ä.) als solche kenntlich gemacht habe. Insbesondere bestätige ich, dass ich *ausnahmslos* und nach bestem Wissen sowohl bei wörtlich übernommenen Aussagen (Zitaten) als auch bei in eigenen Worten wiedergegebenen Aussagen anderer Autorinnen oder Autoren (Paraphrasen) die Urheberschaft angegeben habe.

Sanktionen

Ich nehme zur Kenntnis, dass Arbeiten, welche die Grundsätze der Selbständigkeitserklärung verletzen – insbesondere solche, die Zitate oder Paraphrasen ohne Herkunftsangaben enthalten, als Plagiat betrachtet werden und die entsprechenden rechtlichen und disziplinarischen Konsequenzen nach sich ziehen können (gemäss §§ 7ff der Disziplinarordnung der Universität Zürich sowie §§ 51ff der Rahmenverordnung für das Studium in den Bachelor- und Master-Studiengängen an der Medizinischen Fakultät der Universität Zürich).

Ich bestätige mit meiner Unterschrift die Richtigkeit dieser Angaben.

Pascal Gantenbein

Zürich, den 8.2.2017

11 Curriculum vitae

Pascal Gantenbein

05.07.1989	Geboren in Bachenbülach, ZH
1996 - 2002	Primarschule, Bommeten, Bronschhofen
2002 – 2004	Sekundarschule, Lindenhof, Wil
2004-2009	Mittelschule, Kantonsschule Wil
2009	Eidgenössische Matur mit Schwerpunkt Wirtschaft und Recht an der Kantonsschule Wil
2010 - 2016	Studium der Humanmedizin an der Universität Zürich
2016	Eidgenössisches Examen Humanmedizin an der Universität Zürich
seit 2017	Assistenzarzt Medizin im Spital Zollikerberg